THE JOURNAL OF BIOLOGICAL CHEMISTRY
Vol. 278, No. 28, Issue of July 11, pp. 25600–25606, 2003
Printed in U.S.A.

Identification of p2y$_9$/GPR23 as a Novel G Protein-coupled Receptor for Lysophosphatidic Acid, Structurally Distant from the Edg Family*

Received for publication, March 14, 2003, and in revised form, April 28, 2003
Published, JBC Papers in Press, April 30, 2003, DOI 10.1074/jbc.M302648200

Kyoko Noguchi, Satoshi Ishii‡, and Takao Shimizu

From the Department of Biochemistry and Molecular Biology, Faculty of Medicine, The University of Tokyo, Core Research for Evolutional Science and Technology (CREST) of Japan Science and Technology Corporation, Hongo, Bunkyo-ku, Tokyo 113-0033, Japan

Lysophosphatidic acid (LPA) is a bioactive lipid mediator with diverse physiological and pathological actions on many types of cells. LPA has been widely considered to elicit its biological functions through three types of G protein-coupled receptors, Edg-2 (endothelial cell differentiation gene-2)/LPA$_1$/vzg-1 (ventricular zone gene-1), Edg-4/LPA$_2$, and Edg-7/LPA$_3$. We identified an orphan G protein-coupled receptor, p2y$_9$/GPR23, as the fourth LPA receptor (LPA$_4$). Membrane fractions of RH7777 cells transiently expressing p2y$_9$/GPR23 displayed a specific binding for 1-oleoyl-LPA with a K_d value of around 45 nM. Competition binding and reporter gene assays showed that p2y$_9$/GPR23 preferred structural analogs of LPA with a rank order of 1-oleoyl- > 1-stearoyl- > 1-palmitoyl- > 1-myristoyl- > 1-alkyl- > 1-alkenyl-LPA. In Chinese hamster ovary cells expressing p2y$_9$/GPR23, 1-oleoyl-LPA induced an increase in intracellular Ca^{2+} concentration and stimulated adenylyl cyclase activity. Quantitative real-time PCR demonstrated that mRNA of p2y$_9$/GPR23 was significantly abundant in ovary compared with other tissues. Interestingly, p2y$_9$/GPR23 shares only 20–24% amino acid identities with Edg-2/LPA$_1$, Edg-4/LPA$_2$, and Edg-7/LPA$_3$, and phylogenetic analysis also shows that p2y$_9$/GPR23 is far distant from the Edg family. These facts suggest that p2y$_9$/GPR23 has evolved from different ancestor sequences from the Edg family.

Lysophosphatidic acid (LPA, 1- or 2-acyl-*sn*-glycero-3-phosphate)[1] is a bioactive phospholipid with diverse physiological actions on many cell types (1, 2). LPA induces mitogenic and/or morphological effects on the cells and has been proposed to be involved in biologically important processes, including neurogenesis, myelination, angiogenesis, wound healing, and cancer progression (1, 3). LPA is present in serum at micromolar concentrations (4). LPA is generated mainly by two different pathways; 1) generation of lysophospholipids such as lysophosphatidylcholine (LPC), lysophosphatidylethanolamine (LPE), and lysophosphatidylserine (LPS) from membrane phospholipids by phospholipase A_2 (PLA_2) or phospholipase A_1, followed by conversion of these lysophospholipids to LPA by lysophospholipase D (5) and 2) generation of phosphatidic acid (PA) from phosphatidylcholine (PC) by phospholipase D, followed by conversion of PA to LPA by specific classes of PLA_2 (6).

It has been demonstrated that cell-surface G protein-coupled receptors mediate the cellular effects of LPA. At least three types of G protein-coupled receptors, Edg-2/LPA$_1$/vzg-1 (7), Edg-4/LPA$_2$ (8), and Edg-7/LPA$_3$ (9), which belong to the Edg (endothelial cell differentiation gene) family, have been identified as specific receptors for LPA. These three G protein-coupled receptors share 50–57% amino acid identities. Several experiments have demonstrated that they can mediate adenylyl cyclase inhibition, mitogen-activated protein kinase activation, phospholipase C activation, and Ca^{2+} mobilization through pertussis toxin-sensitive ($G_{i/o}$) and -insensitive G proteins ($G_{12/13}$ and $G_{q/11/14}$) (2, 3). Edg-4/LPA$_2$ and Edg-7/LPA$_3$ have also been shown to activate adenylyl cyclase when they were overexpressed in Sf9 insect cells (9). However, the existence of one or more additional LPA receptors has been implied from the analysis of Edg-2/LPA$_1^{(-/-)}$ Edg-4/LPA$_2^{(-/-)}$ double knockout mice (10) and various pharmacological studies (11–13).

During a "de-orphaning" project of G protein-coupled receptors, we found that p2y$_9$/GPR23 responded to LPA. p2y$_9$/GPR23 specifically bound to LPA and mediated LPA-induced adenylyl cyclase stimulation and intracellular Ca^{2+} mobilization. Although p2y$_9$/GPR23 shares only 20–24% amino acid identities with Edg-2/LPA$_1$, Edg-4/LPA$_2$, and Edg-7/LPA$_3$, and the phylogenetic analysis also shows that p2y$_9$/GPR23 is distant from the Edg family (Fig. 1), our results consistently indicate that p2y$_9$/GPR23 is the fourth LPA receptor (LPA$_4$).

EXPERIMENTAL PROCEDURES

Materials and Cells—1-Myristoyl (14:0), -palmitoyl (16:0), -stearoyl (18:0), and -oleoyl (18:1)-LPAs, 18:1-LPC, 18:1-LPE, 18:1-lysophosphatidylglycerol (LPG), and 18:1-LPS were purchased from Avanti Polar Lipids (Alabaster, AL). 18:1-LPA was also purchased from Cayman

* This work was supported by grants-in-aid from the Ministry of Education, Science, Culture, Sports and Technology of Japan (to T. S. and S. I.), grants-in-aid for Comprehensive Research on Aging and Health, and Research on Allergic Disease and Immunology from the Ministry of Health, Labour, and Welfare, Japan, and grants from the Yamanouchi Foundation for Research on Metabolic Disorders, the Kanae Foundation for Life and Socio-medical Science, and the Uehara Memorial Foundation (to S. I.). The costs of publication of this article were defrayed in part by the payment of page charges. This article must therefore be hereby marked "*advertisement*" in accordance with 18 U.S.C. Section 1734 solely to indicate this fact.

‡ To whom correspondence should be addressed. Tel.: 81-3-5802-2925; Fax: 81-3-3813-8732; E-mail: mame@m.u-tokyo.ac.jp.

[1] The abbreviations used are: LPA, lysophosphatidic acid; LPC, lysophosphatidylcholine; LPE, lysophosphatidylethanolamine; LPS, lysophosphatidylserine; PLA_2, phospholipase A_2; PA, phosphatidic acid; PC, phosphatidylcholine; 14:0, 1-myristoyl; 16:0, 1-palmitoyl; 18:0, 1-stearoyl; 18:1, 1-oleoyl; LPG, lysophosphatidylglycerol; PAF, platelet-activating factor; S1P, sphingosine 1-phosphate; SPC, sphingosylphosphorylcholine; BSA, bovine serum albumin; DMEM, Dulbecco's modified Eagle's medium; HA, hemagglutinin; CHO, Chinese hamster ovary; HBSS, Hanks' balanced salt solution; $[Ca^{2+}]_i$, intracellular Ca^{2+} concentration; GAPDH, glyceraldehyde-3-phosphate dehydrogenase; EST, expressed sequence tag.

Chemical (Ann Arbor, MI). 1-Alkyl- and 1-alkenyl-LPAs were kind gifts from Dr. R. Taguchi (Nagoya City University, Japan), which were prepared from bovine heart lyso-platelet-activating factor (lyso-PAF) and lyso-plasmalogen, respectively, by using phospholipase D. 18:1-PA and 17 nucleotides (ADP-glucose, ATP, ADP, *S*-adenosyl-L-methionine, *S*-adenosyl-L-homocysteine, CTP, GDP-fucose, GDP-mannose, GDP, UDP, UDP-*N*-acetylglucosamine, UDP-galactose, UDP-glucose, UDP-*N*-acetylgalactosamine, UTP, UDP-glucuronic acid, and GTP) were from Sigma (St. Louis, MO). Sphingosine 1-phosphate (S1P) and the Bioactive Lipid Library were from Biomol Research Laboratories (Plymouth Meeting, PA). Sphingosylphosphorylcholine (SPC) and 1-*O*-hexadecyl-PAF were from Cayman Chemical. [^{3}H]LPA (1-oleoyl[oleoyl-9,10-^{3}H(N)]LPA, 57 Ci/mmol) was from PerkinElmer Life Sciences (Boston, MA). Bovine serum albumin (BSA) from Serologicals Proteins (Kankakee, IL) was of fatty acid-free and very low endotoxin grade. Other chemical reagents were of analytical grade. RH7777 rat hepatoma cells and B103 rat neuroblastoma cells were kindly provided from Dr. J. Chun (University of California-San Diego, La Jolla, CA). Human megakaryoblastic MEG-01 cells were purchased from the Health Science Research Resources Bank (Osaka, Japan).

Construction of the Phylogenetic Tree—Peptide sequences of selected G protein-coupled receptors were obtained from GenBank™ and SwissProt. The phylogenetic tree was generated from peptide sequences of selected G protein-coupled receptors, using the all-against-all matching method (available at cbrg.inf.ethz.ch/Server/AllAll.html). The tree was constructed on the basis of point-accepted mutation distances between each pair of sequences estimated by the dynamic programming algorithm.

Cloning of p2y$_9$/GPR23—The tBLASTn program was used to search the data base of GenBank™ for orphan G protein-coupled receptors sharing high identities with the human PAF receptor (14). A DNA fragment containing the entire open reading frame of p2y$_9$/GPR23 (GenBank™ accession number NM_005296) was first amplified from human genomic DNA by PCR using KOD-Plus (Toyobo, Osaka, Japan) and oligonucleotides (sense primer, 5′-GTCCATAGTGTCAGAGTGGTGAAC-3′; antisense primer, 5′-CATATCTGGACCTGAACACATTTC-3′). The entire open reading frame of p2y$_9$/GPR23 with an additional sequence of hemagglutin (HA)-epitope at the 5′-end was subsequently amplified from the resultant PCR products using KOD-Plus and oligonucleotides (sense primer containing *Kpn*I and HA tag sequences, 5′-GGGGTACCGCCATGTACCCCTACGACGTGCCCGACTACGCCGGTGACAGAAGATTCATT-3′; antisense primer containing *Xba*I sequence, 5′-GCTCTAGACTAAAAGGTGGATTCTAG-3′). The resultant DNA fragment was digested with *Kpn*I and *Xba*I and subsequently cloned into the mammalian expression vector pCXN2.1, a slightly modified version of pCXN2 (15) with multiple cloning sites, between *Kpn*I and *Nhe*I sites.

Binding Assay—RH7777 cells and B103 cells were cultured on collagen-coated dishes in Dulbecco's modified Eagle's medium (DMEM, Sigma) supplemented with 10% fetal bovine serum (Cambrex Co., Walkersville, MD), 100 IU/ml penicillin, and 100 μg/ml streptomycin (Roche Applied Science). Cells were transfected with p2y$_9$/GPR23-pCXN2.1 or empty vector using LipofectAMINE 2000 reagent (Invitrogen). After 24 h of transfection, cells were washed with phosphate-buffered saline three times and serum-starved for 24 h in DMEM supplemented with 0.1% BSA. The cells were washed again with phosphate-buffered saline twice and scraped off. After further washing with binding buffer (25 mM HEPES-NaOH (pH 7.4), 10 mM $MgCl_2$, and 0.25 M sucrose), the cells were suspended in the buffer with additional 20 μM 4-amidinophenylmethylsulfonyl fluoride (Sigma) and a protease inhibitor mixture (Complete, Roche Applied Science), sonicated three times at 15 watts for 30 s, and centrifuged at 800 × *g* for 10 min at 4 °C. The supernatant was further centrifuged at 10^5 × *g* for 60 min at 4 °C, and the resultant pellet was homogenized in ice-cold binding buffer. Binding assays were performed in 96-well plates in triplicates. For Scatchard analysis, 40 μg of the membrane fractions were incubated in binding buffer containing 0.25% BSA with various concentrations of [^{3}H]LPA for 60 min at 4 °C. The bound [^{3}H]LPA was collected onto a Unifilter-96-GF/C (PerkinElmer Life Sciences) using a MicroMate 196 harvester (Packard, Wellesley, MA). The filter was then rinsed ten times with binding buffer containing 0.25% BSA and dried for 2 h at 50 °C. 25 μl of MicroScint-0 scintillation mixture (PerkinElmer Life Sciences) was added per well. The radioactivity that remained on the filter was measured with a TopCount microplate scintillation counter (Packard). Total and nonspecific bindings were evaluated in the absence and presence of 10 μM unlabeled LPA, respectively. The specific binding value (dpm) was calculated by subtracting the nonspecific binding value (dpm) from the total binding value (dpm). For competition assay with related lipids, 20 μg of the membrane fractions were incubated with 5 nM [^{3}H]LPA in the absence or presence of 1 μM of unlabeled 18:1-LPA, 18:1-LPC, 18:1-LPE, 18:1-LPS, 18:1-LPG, 18:1-PA, PAF, S1P, or SPC. For competition assay with structural analogs of LPA, 10 μg of the membrane fractions was incubated with increasing concentrations of unlabeled 18:1-, 18:0-, 1-alkyl-, and 1-alkenyl-LPA in the presence of 2.5 nM [^{3}H]LPA. Before conducting the binding assays, the cell surface expression of p2y$_9$/GPR23 was confirmed by flow cytometric analysis (Epics XL, Beckman Coulter, Fullerton, CA) with anti-HA rat IgG (3F10, Roche Applied Science) and phycoerythrin-labeled anti-rat IgG (Beckman Coulter) as the second antibody.

Reporter Gene Assay—PC-12 cells were cultured in DMEM supplemented with 10% horse serum and 5% fetal bovine serum. 2 × 10^5 cells were transfected with 450 ng of p2y$_9$/GPR23-pCXN2.1 or empty vector, 530 ng of *zif* 268-firefly luciferase-pGL2 (a kind gift from Dr. T. Naito, Japan Tobacco, Tokyo, Japan), and 20 ng of CMV-*Renilla* luciferase-pRL (Promega, Madison, WI) using SuperFect (Qiagen, Hiden, Germany), and cultured on collagen-coated 24-well plates for 48 h. Cells were washed three times with DMEM supplemented with 0.1% BSA and cultured in the serum-free DMEM for 12 h, and stimulated with various concentrations of LPA analogs. Firefly and *Renilla* luciferase activities were measured using PICAGENE Dual Seapansy (Toyo Ink, Tokyo, Japan) and a MiniLumat LB 9506 luminometer (Berthold, Bundoora, Australia). Firefly luciferase values were standardized to *Renilla* ones.

Ca^{2+} Measurement—Chinese hamster ovary (CHO) cells were cultured in Ham's F-12 (Sigma) supplemented with 10% fetal bovine serum, 100 IU/ml penicillin, and 100 μg/ml streptomycin. Cells were transfected with p2y$_9$/GPR23-pCXN2.1 or empty vector using LipofectAMINE 2000 reagent. Stably transfected clones were selected with 2 mg/ml G418 (Invitrogen, Carlsbad, CA) and maintained with 0.3 mg/ml G418. Cell surface expression of p2y$_9$/GPR23 was detected by flow cytometric analysis as described above (see Fig. 4*A*). For the ligand screening assay, clones highly expressing p2y$_9$/GPR23 were seeded in 96-well plates at a density of 4 × 10^4 cells/well and cultured overnight. They were loaded with 4 μM Fluo-3 AM (Dojindo, Kumamoto, Japan) in HEPES-HBSS buffer (1 × Hanks' balanced salt solution (HBSS) containing 20 mM HEPES-NaOH (pH 7.4), 1 mM $CaCl_2$, 0.5 mM $MgCl_2$, 0.1% BSA, and 2.5 mM probenecid) and 0.04% pluronic acid for 1 h at 37 °C, washed twice, and filled with HEPES-HBSS buffer. They were then stimulated with 198 lipids contained in the Bioactive Lipid Library and 17 nucleotides (described under "Materials and Cells") individually, and intracellular Ca^{2+} mobilization was monitored with a scanning fluorometer (FLEXstation, Molecular Devices, Sunnyvale, CA) at an excitation wavelength of 485 nm and an emission wavelength of 525 nm. For examination of dose dependence, CHO cell clones highly expressing p2y$_9$/GPR23 or mock-transfected cells were washed with phosphate-buffered saline three times, serum-starved for 24 h in Ham's F-12 supplemented with 0.1% BSA, washed twice again with phosphate-buffered saline, and then harvested. The harvested cells were further washed with HEPES-Tyrode's buffer (25 mM HEPES-NaOH (pH 7.4), 140 mM NaCl, 2.7 mM KCl, 1 mM $CaCl_2$, 0.49 mM $MgCl_2$, 12 mM $NaHCO_3$, 0.37 mM NaH_2PO_4, and 5.6 mM D-glucose), and loaded with 3 μM Fura-2 AM (Dojindo) in HEPES-Tyrode's buffer containing 0.1% BSA (HEPES-Tyrode's BSA buffer) for 1 h at 37 °C. Cells were washed twice and resuspended in HEPES-Tyrode's BSA buffer at a density of 2 × 10^6 cells/ml. 0.5 ml of the cell suspension was applied to a CAF-100 spectrofluorometer (Jasco, Tokyo, Japan), and 5 μl of various concentrations of 18:1-LPA in HEPES-Tyrode's BSA buffer was added. Intracellular Ca^{2+} concentration ($[Ca^{2+}]_i$) was measured by the ratio of emission fluorescence of 500 nm by excitations at 340 and 380 nm.

cAMP Assay—CHO cell clones stably expressing p2y$_9$/GPR23 were used to measure cAMP levels. After 24 h of serum starvation, cells were harvested and suspended in HBSS containing 0.1% BSA and 0.5 mM isobutylmethylxanthine. The density was 5 × 10^6 or 5 × 10^7 cells/ml for assay in the presence or absence of forskolin, respectively. 20 μl of the cell suspension was applied to 96-well plates and incubated for 20 min at room temperature. The reaction was initiated by adding 10 μl of ligand solution of 18:1-LPA in HBSS-BSA buffer with or without 5 μM forskolin. After 30 min of incubation at room temperature, the reaction was terminated by adding 10 μl of HBSS-BSA buffer containing 4% Tween 20. After centrifugation at 800 × *g* for 5 min, cAMP contents in the supernatant were measured by a Fusion system (Packard) using an AlphaScreen cAMP assay kit (PerkinElmer Life Sciences). Pretreatment with pertussis toxin (List Biological Laboratories, Campbell, CA) was for 12 h at a concentration of 100 ng/ml. Results were expressed as -fold increases over respective controls.

Quantitative Real-time PCR—Human first strand cDNAs from 16 tissues were purchased from Clontech (Human MTC Panel I and II),

whose concentrations were normalized to the mRNA expression levels of four different housekeeping genes (α-tubulin, β-actin, glyceraldehyde-3-phosphate dehydrogenase (GAPDH), and PLA_2). The cDNA levels of GAPDH and $p2y_9$/GPR23 were quantified using a LightCycler apparatus (Roche Applied Science). The PCR reactions were set up in microcapillary tubes in a volume of 20 μl, consisting of 2 μl of cDNA solution, 1× FastStart DNA Master SYBR Green I (Roche Applied Science), 0.5 μM each sense and antisense primers and 3 mM $MgCl_2$. The PCR program for GAPDH was as follows; denaturation at 95 °C for 3 min and 50 cycles of amplification consisting of denaturation at 95 °C for 0 s, annealing at 60 °C for 5 s, and extension at 72 °C for 40 s. The PCR program for $p2y_9$/GPR23 was as follows: denaturation at 95 °C for 5 min and 50 cycles of amplification consisting of denaturation at 95 °C for 15 s, annealing at 60 °C for 5 s, and extension at 72 °C for 6 s. For GAPDH, a human GAPDH control Amplimer Set (Clontech), designed to amplify a 983-bp fragment was used as primers; sense primer: 5′-TGAAGGTCGGAGTCAACGGATTTGGT-3′ and antisense primer: 5′-CATGTGGGCCATGAGGTCCACCAC-3′. The primers for $p2y_9$/GPR23 were designed to amplify a 139-bp fragment; sense primer: 5′-AAAGATCATGTACCCAATCACCTT-3′ and antisense primer: 5′-CTTAAACAGGGACTCCATTCTGAT-3′. The PCR products were detected by measuring the fluorescence of SYBR Green I, which selectively bound to double-stranded DNA and emitted the greatly enhanced fluorescence. The cDNA level of each sample was quantified by Fit Points Method in LightCycler analysis software. The control cDNA contained in Clontech human MTC Panels and a linearized $p2y_9$/GPR23-pCXN2.1 were used as standards for GAPDH and $p2y_9$/GPR23, respectively. In both cases, the quality of PCR products was assessed by monitoring a fusion step.

Northern Hybridization—Human poly(A)$^+$ RNA samples from kidney and skeletal muscle were purchased from Clontech. Total RNA of human megakaryoblastic MEG-01 cells was extracted with Absolutely RNA RT-PCR Miniprep kit (Stratagene, La Jolla, CA). Poly(A)$^+$ RNA was isolated from 200 μg of the total RNA using μMACS mRNA isolation kit (Miltenyi Biotec, Bergisch Gladbach, Germany). For Northern analysis, 2.5 μg of poly(A)$^+$ RNA was hybridized with [^{32}P]dCTP-labeled probes of human $p2y_9$/GPR23 and human β-actin, as described previously (16). The washed membrane was subjected to autoradiography for 4 days ($p2y_9$/GPR23) or 3 h (β-actin).

RESULTS

Screening of Candidate Ligands—Phylogenetic analysis showed that $p2y_9$/GPR23 was most closely related to the orphan receptor $p2y_5$ and relatively close to the functional receptors for nucleotides ($P2Y_1$, $P2Y_4$, and $P2Y_6$) (17) and for lipids (G2A, GPR4, GPR65/TDAG8, GPR68/OGR1, PAF receptor, $CysLT_1$, and $CysLT_2$) (18) (Fig. 1). It was, therefore, supposed that $p2y_9$/GPR23 might interact with lipids or nucleotides. We screened 198 lipids and 17 nucleotides using CHO cells stably expressing $p2y_9$/GPR23 by measuring intracellular Ca^{2+} mobilization with FLEXstation, a scanning fluorometer. Among them, 18:1-LPA at a concentration of 10 μM induced a significant increase in $[Ca^{2+}]_i$ in $p2y_9$/GPR23-expressing cells, but not in $p2y_5$-expressing cells (data not shown).

Membrane Binding Assay—To characterize the binding of LPA to $p2y_9$/GPR23, we conducted membrane binding assays using [^{3}H]18:1-LPA. RH7777 rat hepatoma cells transiently transfected with $p2y_9$/GPR23 were used, because RH7777 cells were not responsive to LPA (19). As expected, membrane fractions of mock-transfected RH7777 cells displayed low background binding of [^{3}H]LPA (Fig. 2*A*). [^{3}H]LPA binding to membrane fractions of RH7777 cells was greatly enhanced by $p2y_9$/GPR23 transfection (Fig. 2*A*). Reverse transcriptase-PCR analyses showed no induction of endogenous receptors (Edg-2/LPA_1, Edg-4/LPA_2, or Edg-7/LPA_3) by $p2y_9$/GPR23 transfection (data not shown). Scatchard analysis indicated a dissociation constant (K_d) of 44.8 nM and a maximum binding capacity (B_{max}) of 37.2 pmol/mg of protein (Fig. 2*B*). Competition analyses revealed that only 18:1-LPA, but not 18:1-LPC, 18:1-LPE, 18:1-LPS, 18:1-LPG, 18:1-PA, PAF, S1P, or SPC competed for [^{3}H]LPA binding to the membrane fractions of $p2y_9$/GPR23-expressing RH7777 cells (Fig. 2*C*). 18:1- and 18:0-LPA competed for [^{3}H]LPA binding to the membrane fractions of $p2y_9$/GPR23-expressing RH7777 cells with K_i values of 80.0 and 282 nM, respectively (Fig. 2*D*). 1-Alkyl- and 1-alkenyl-LPA also competed for [^{3}H]LPA binding but rather weakly (Fig. 2*D*). Because B103 rat neuroblastoma cells were also reported to lack responsiveness to LPA (19), binding assays using B103 cells were performed in the same manner as RH7777 cells. The specific binding activities of $p2y_9$/GPR23-transfected B103 cells were 289, 859, and 2975 dpm/50 μg of protein at 1, 3, and 10 nM [^{3}H]LPA, respectively. Based on the specific activity of [^{3}H]LPA, 2975 dpm/50 μg of protein corresponds to 0.47 pmol/mg of protein. The binding activities of the mock-transfected B103 cells were 79, 197, and 238 dpm/50 μg of protein at 1, 3, and 10 nM [^{3}H]LPA, respectively.

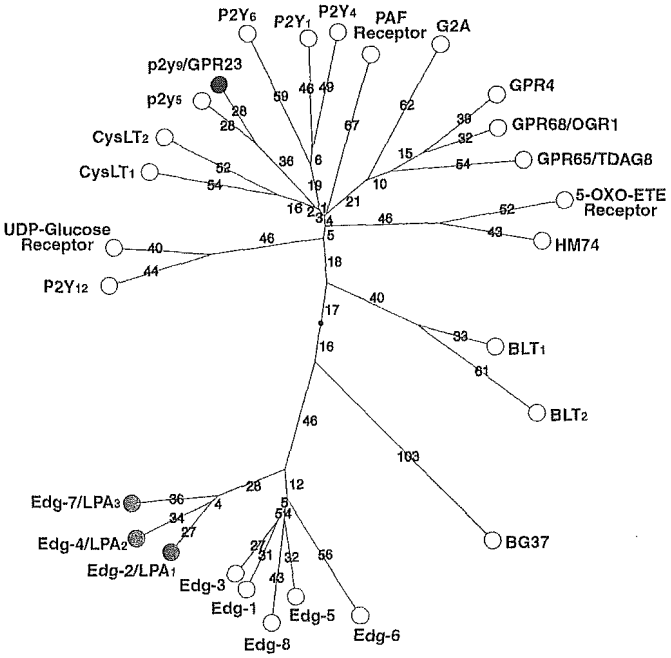

FIG. 1. **Phylogenetic tree constructed for $p2y_9$/GPR23 and selected human G protein-coupled receptors.** Values show branch lengths that represent the evolutionary distance between each pair of sequences. The sequence divergence is equal to the sum of each value of branch length. A *small dot* indicates the weighted centroid of the tree.

Reporter Gene Assay—We next performed reporter gene assays to examine the ligand preference of $p2y_9$/GPR23. The transfected PC-12 cells responded to all LPA analogs with a significant increase in the luciferase activity in a dose-dependent manner; 18:1-LPA evoked the highest activity, followed by 18:0-, 16:0-, and 14:0-derivatives (Fig. 3). Compared with 1-acyl-LPAs, 1-alkyl-, and 1-alkenyl-LPA exhibited weaker activities. Mock-transfected PC-12 cells showed no responses to any analogs of LPA (data not shown).

Effect on Intracellular Ca^{2+} Mobilization—To characterize the intracellular signals of $p2y_9$/GPR23, the effect of LPA on intracellular Ca^{2+} mobilization was examined in detail using a CAF-100 spectrofluorometer. We established four independent clones of CHO cells stably expressing $p2y_9$/GPR23 and a polyclonal population of mock-transfected CHO cells. Cell surface expression of $p2y_9$/GPR23 was confirmed by flow cytometric analysis (Fig. 4*A*). The other three clones showed similar expression patterns. Either in $p2y_9$/GPR23-expressing or mock-transfected CHO cells, 18:1-LPA induced an increase in $[Ca^{2+}]_i$ in a dose-dependent manner (Fig. 4*B*). Although mock-transfected CHO cells displayed a significant increase in $[Ca^{2+}]_i$, the increase in $[Ca^{2+}]_i$ was enhanced ~2-fold by the stable expression of $p2y_9$/GPR23. Similar results were obtained in all four different clones. The effects of 18:1-LPA were reproducibly

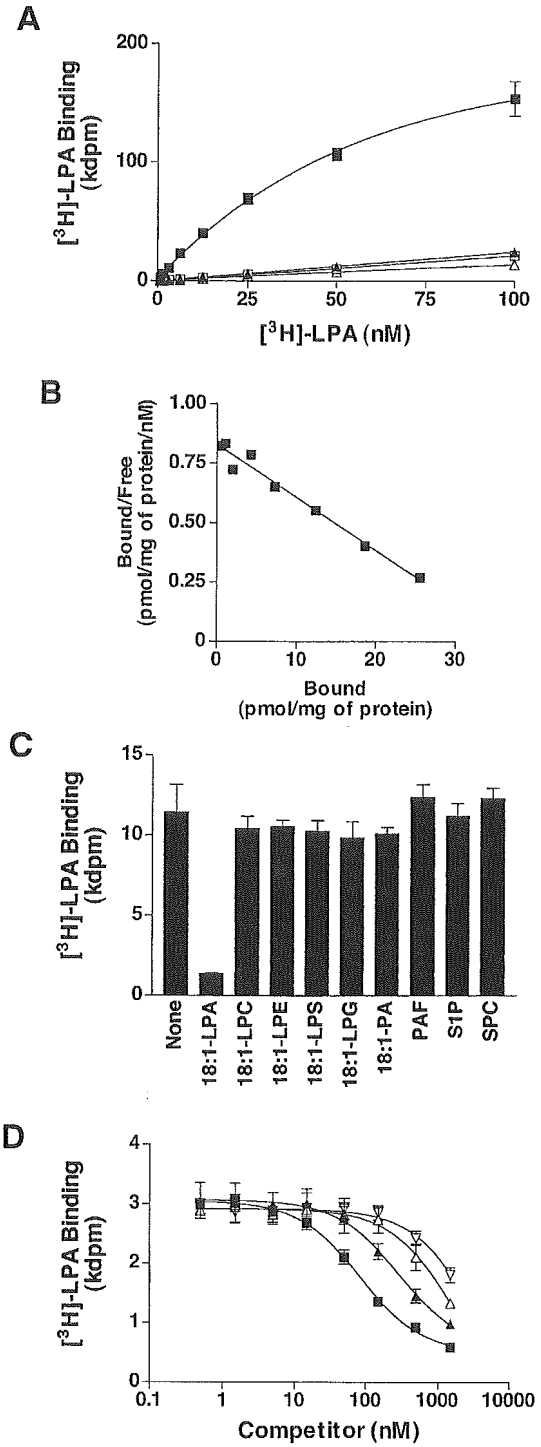

FIG. 2. **[^{3}H]LPA binding to RH7777 cell membranes.** *A*, [^{3}H]LPA binding to p2y$_9$/GPR23. Membrane fractions of RH7777 cells transiently expressing p2y$_9$/GPR23 (*closed symbols*) and mock-transfected cells (*open symbols*) were incubated with increasing concentrations of [^{3}H]18:1-LPA in the presence or absence of 10 μM unlabeled 18:1-LPA. Total binding (■ and □) and nonspecific binding (▲ and △) are presented. Data are means ± S.D. (n = 3). *B*, Scatchard analysis of the specific binding of [^{3}H]LPA to p2y$_9$/GPR23. *C*, competition for [^{3}H]LPA binding with related lipids. Membrane fractions of RH7777 cells transiently expressing p2y$_9$/GPR23 were incubated with 5 nM [^{3}H]18:1-LPA in the presence of 1 μM unlabeled lipids. The total amounts of [^{3}H]LPA bound are presented. Data are means ± S.D. (n = 3) of a representative of two independent experiments. *D*, competition for [^{3}H]LPA binding with structural analogs of LPA. Membrane fractions of RH7777 cells transiently expressing p2y$_9$/GPR23 were incubated with increasing concentrations of unlabeled 18:1- (■), 18:0- (▲), 1-alkyl- (△), and 1-alkenyl- (▽) LPA in the presence of 2.5 nM [^{3}H]18:1-LPA. The total amounts of [^{3}H]LPA bound are presented. Data are means ± S.D. (n = 3) of a representative of two independent experiments.

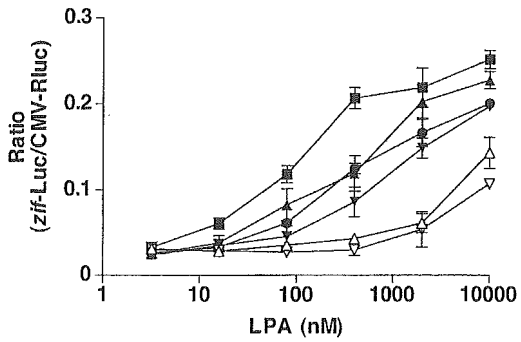

FIG. 3. **Induction of reporter gene expression by structural analogs of LPA in PC-12 cells.** PC-12 cells were transiently transfected with the reporter plasmids containing the *zif* 268 promoter-driven firefly luciferase gene and the control plasmid containing the cytomegalovirus promoter-driven *Renilla* luciferase gene together with the p2y$_9$/GPR23 expression plasmid. Cells were stimulated with increasing concentrations of 18:1- (■), 18:0- (▲), 16:0- (●), 14:0- (▼), 1-alkyl- (△), and 1-alkenyl- (▽) LPA. The ratios of firefly luciferase activity to *Renilla* one are shown. Data are means ± S.D. (n = 3) of a representative of two independent experiments.

observed, using different batches of the LPA from two companies (Cayman and Avanti). In B103 cells transiently expressing p2y$_9$/GPR23, 18:1-LPA at concentrations of 1 and 10 nM evoked increases in $[Ca^{2+}]_i$ by 38 ± 5 and 49 ± 5 nM (mean ± S.D.; n = 3), respectively. Mock-transfected B103 cells showed no response at 10 nM 18:1-LPA. On the other hand, RH7777 cells were unresponsive to 18:1-LPA both in mock-transfected and in p2y$_9$/GPR23-expressing form (data not shown).

Effect on cAMP Formation—18:1-LPA induced an increase in cAMP levels in p2y$_9$/GPR23-expressing CHO cells either in the absence or presence of 5 μM forskolin (Fig. 5, *A* and *B*), and pretreatment of the cells with pertussis toxin further increased the cAMP levels (Fig. 5, *A* and *B*). In mock-transfected CHO cells, LPA induced no change or a decrease in cAMP levels in the absence or presence of forskolin, respectively (Fig. 5, *A* and *B*), and pretreatment of the cells with pertussis toxin attenuated an LPA-induced decrease in cAMP levels (Fig. 5*B*).

Tissue Distribution—To explore the physiological function of p2y$_9$/GPR23 *in vivo*, it is important to know the tissue distribution of the receptor. By using cDNAs prepared from 16 human tissues as templates, quantitative real-time PCR was performed to estimate the mRNA expression levels. In a set of samples, ovary showed the highest expression of p2y$_9$/GPR23 mRNA, whereas other tissues showed only weak expressions (Fig. 6*A*). Northern hybridization of human poly(A)$^+$ RNA from kidney, skeletal muscle, and megakaryoblastic MEG-01 cells (20) detected a transcript of about 4.4 kb (Fig. 6*C*).

DISCUSSION

LPA is a lipid mediator with diverse physiological activities (1, 3). Many structural analogs of LPA have been identified in mammalian cells and tissues. Most are 1-acyl-LPAs with unsaturated fatty acyl-chains (oleoyl, linoleoyl, and arachidonoyl), and smaller amounts are with saturated fatty acyl-chains (palmitoyl and stearoyl) (21). Recently, 1-alkyl-, 1-alkenyl-, and 2-acyl-LPAs were also found (22–24). LPA has been widely considered to elicit its physiological functions through three types of G protein-coupled receptors, Edg-2/LPA$_1$, Edg-4/LPA$_2$, and Edg-7/LPA$_3$ (2, 3). However, there are some reports implying the existence of an additional LPA receptor(s). First, in the study of Edg-2/LPA$_1^{(-/-)}$ Edg-4/LPA$_2^{(-/-)}$ double knockout mice, some LPA-induced responses, such as inositol phosphate production, adenylyl cyclase inhibition, and stress fiber formation, were absent or severely reduced but still remained at high LPA concentrations in embry-

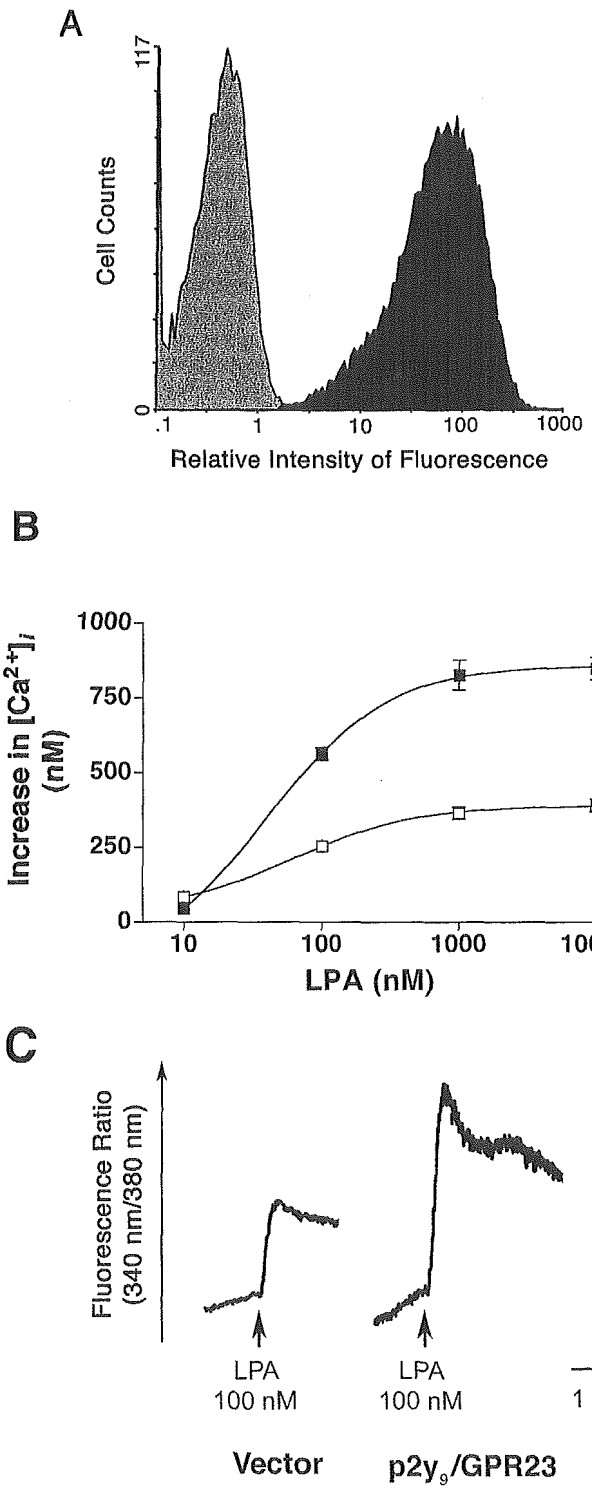

FIG. 4. **LPA-induced increase in $[Ca^{2+}]_i$ in CHO cells.** *A*, cell surface expression of $p2y_9$/GPR23. In a clonal population of CHO cells stably expressing $p2y_9$/GPR23 tagged with HA at N terminus (*black area*), the higher intensity of fluorescence was detected by flow cytometric analysis than in mock-transfected CHO cells (*gray area*). This is a representative result of four independent clones, which gave essentially identical patterns. *B*, dose-response curves. A clonal population of CHO cells stably expressing $p2y_9$/GPR23 was loaded with 3 μM Fura-2 AM, and stimulated with increasing concentrations of 18:1-LPA (■). The results of mock-transfected CHO cells are also shown as a negative control (□). Data are means ± S.D. (n = 3) of a representative of four different stable clones. *C*, representative traces of Ca^{2+} responses. A clonal population of CHO cells stably expressing $p2y_9$/GPR23 was stimulated with 100 nM 18:1-LPA (*right*). A result of mock-transfected CHO cells is also shown as a negative control (*left*).

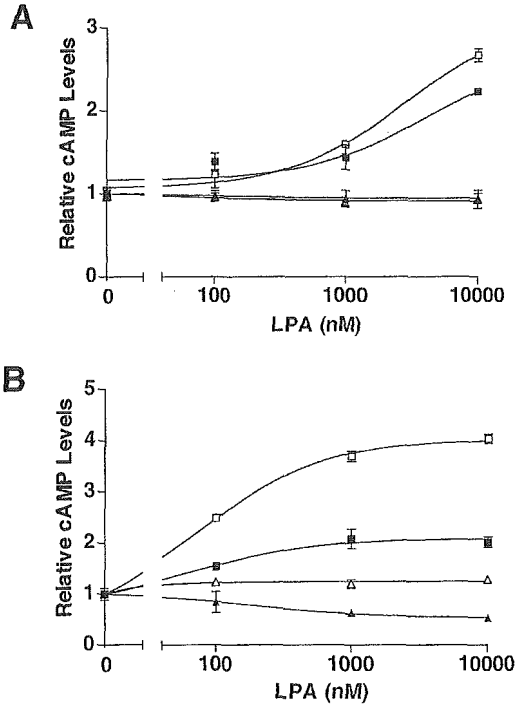

FIG. 5. **Effects of LPA on cAMP accumulation in CHO cells.** *A*, dose-response curves. A clonal population of CHO cells stably expressing $p2y_9$/GPR23 was stimulated with increasing concentrations of 18:1-LPA in the presence of 0.5 mM isobutylmethylxanthine. The cAMP contents are presented (■). The effect of pertussis toxin pretreatment on cAMP accumulation is also shown (□). The results of mock-transfected CHO cells are displayed as a negative control (▲, pertussis toxin-untreated cells; △, pertussis toxin-treated cells). cAMP levels are expressed as -fold increases above basal contents. Data are means ± S.D. (n = 4). *B*, effects of forskolin on cAMP accumulation. Cells were stimulated with 18:1-LPA in the presence of 5 μM forskolin. Assay was performed in the same manner as *A*. *Symbols* are expressed as in *A*. Data are means ± S.D. (n = 4).

onic fibroblast cells (10). They reported that Edg-7/LPA_3 was not detected by Northern blotting or reverse transcriptase-PCR in these cells. Second, RH7777 cells that do not express Edg-2/LPA_1, Edg-4/LPA_2, or Edg-7/LPA_3 have a mitogenic response to LPA and LPA analogs (12). Third, LPA-induced platelet aggregation showed different ligand specificities with Edg receptor-mediated response; the platelet response lacks the stereoselectivity (11), requires micromolar concentrations of LPA (11), and displays a distinct ligand selectivity with a preference to 1-alkyl-LPAs (13). Here we identified $p2y_9$/GPR23 as the fourth LPA receptor (LPA_4).

$p2y_9$/GPR23 was identified as a novel G protein-coupled receptor from an analysis of the expressed sequence tag (EST) data base, and the complete clone was isolated from human genomic DNA (25, 26). The $p2y_9$/GPR23 gene is located on chromosome X, region q13-q21.1, and contains an intronless open reading frame of 1113 bp encoding 370 amino acids (25, 26). However, information is limited regarding the specific ligands, tissue distribution, and biological functions of this orphan receptor.

Membrane fractions of RH7777 cells transiently transfected with $p2y_9$/GPR23 had a specific binding activity for 18:1-LPA with a K_d value of 44.8 nM (Fig. 2, *A* and *B*). Competition assays displayed the binding affinity with a rank order of 18:1- > 18:0- > 1-alkyl- > 1-alkenyl-LPA (Fig. 2*D*). This order was consistent with that of the luciferase activity: 18:1- > 18:0- > 16:0- > 14:0- > 1-alkyl- > 1-alkenyl-LPA (Fig. 3). These results indicate that 1-acyl-LPA is a better ligand for $p2y_9$/GPR23 than 1-alkyl- or 1-alkenyl-LPA, like the

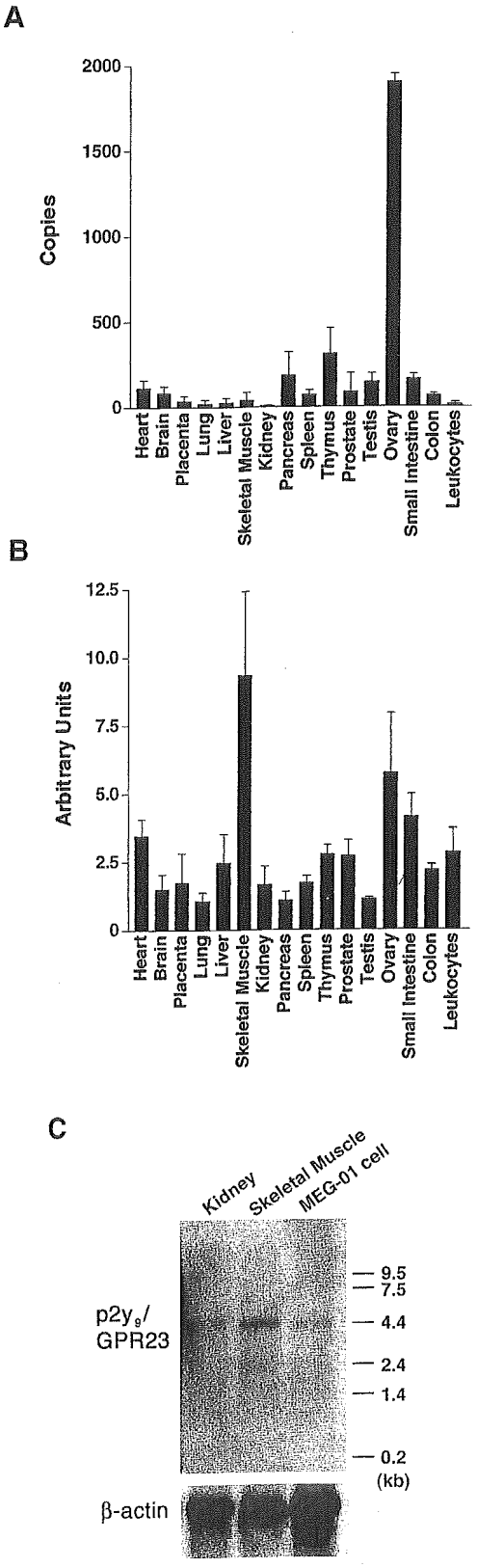

FIG. 6. **Expression of p2y$_9$/GPR23 mRNA.** *A*, quantitative real-time PCR in 16 human tissues. Expression levels of p2y$_9$/GPR23 mRNA are presented with the number of cDNA molecules initially involved in 2 μl of the template solutions. *Bars* show the mean ± S.D. of three independent experiments. *B*, expression levels of GAPDH mRNA. Quantitative real-time PCR was performed for GAPDH mRNA. Data are presented in arbitrary units. *Bars* show the means ± S.D. of three independent experiments. *C*, Northern blot analysis. Human poly(A)$^+$ RNAs (2.5 μg) were electrophoretically separated, transferred to a nylon membrane, and hybridized sequentially with [^{32}P]dCTP-labeled probes of human p2y$_9$/GPR23 and human β-actin.

previously identified LPA receptors (Edg-2/LPA$_1$, Edg-4/LPA$_2$, and Edg-7/LPA$_3$) (27, 28). Furthermore, Im *et al.* (29) showed that, among 1-acyl-LPAs, 18:1-LPA was more active than 18:0-, 16:0-, and 14:0-LPA in [γ-^{35}S]GTP binding assay with Edg-4/LPA$_2$ and Edg-7/LPA$_3$.

Mock-transfected CHO cells displayed an increase in $[Ca^{2+}]_i$ (Fig. 4, *B* and *C*), possibly due to the presence of endogenous LPA receptors. Despite this background response of CHO cells, the stable expression of p2y$_9$/GPR23 significantly enhanced the LPA-induced Ca^{2+} response by ~2-fold (Fig. 4*B*) in four independent clones. These results strongly suggest that p2y$_9$/GPR23 could elicit an intracellular Ca^{2+} mobilization, a well documented cellular effect of LPA (27).

In mock-transfected CHO cells, LPA induced a decrease in cAMP levels in the presence of forskolin, which was inhibited by pretreatment of the cells with pertussis toxin (Fig. 5*B*), suggesting the existence of endogenous LPA receptors coupling with pertussis toxin-sensitive G protein ($G_{i/o}$). By contrast, LPA induced an increase in cAMP levels in p2y$_9$/GPR23-expressing CHO cells, and pretreatment of the cells with pertussis toxin further potentiated the LPA-induced cAMP accumulation (Fig. 5, *A* and *B*). It is, therefore, possible that p2y$_9$/GPR23 is coupled with G_s, and that the effect of LPA on p2y$_9$/GPR23 is unmasked by blocking the pertussis toxin-sensitive signals from endogenous LPA receptors in CHO cells. Muscarinic M_2 and somatostatin sst_5 receptors are coupled with G_i, inhibiting adenylyl cyclase in CHO cells. However, at higher agonist concentrations, these receptors can also mediate activation of adenylyl cyclase by a mechanism involving G_s activation (30, 31). Conversely, at lower concentrations of LPA, p2y$_9$/GPR23 might inhibit the production of cAMP via G_i, like Edg-2/LPA$_1$, Edg-4/LPA$_2$, and Edg-7/LPA$_3$ (2, 3).

We also found that forskolin facilitated LPA-induced cAMP accumulation in p2y$_9$/GPR23-expressing CHO cells (Fig. 5, *A* and *B*). At least ten types of mammalian adenylyl cyclase are at present identified (32). All types of adenylyl cyclase are activated by G_s and by forskolin, and some types of adenylyl cyclase (type II, IV, V, and VI) are synergistically activated in the presence of both G_s and forskolin (32). One possible explanation of our results is that the latter types of adenylyl cyclase might be involved in the LPA-induced cAMP accumulation in p2y$_9$/GPR23-expressing CHO cells. Indeed, type VI and type VII adenylyl cyclases are expressed in CHO cells (33).

The mRNA levels of p2y$_9$/GPR23 were significantly high in ovary (Fig. 6). Various species of LPA such as linoleic, arachidonic, and docosahexaenoic acids were detected from ascites of ovarian cancer patients (24), and they had many effects on the ovarian cancer progression such as cell proliferation, prevention of apoptosis, resistance to cisplatin, and production of vascular endothelial growth factor (34). Consistently, a prominent expression of Edg-4/LPA$_2$ has been shown in primary cultures and established lines of ovarian cancer cells (35). LPA was also found at relatively high concentrations in human ovarian follicular fluid from healthy subjects (36), suggesting the relevance of LPA for normal ovarian functions as well. Tokumura (37) recently described in his review article that LPA increased the intracellular cAMP level in mouse cumulus cells. This phenomenon is consistent with our findings that the activation of p2y$_9$/GPR23 evoked cAMP accumulation in CHO cells. Thus, p2y$_9$/GPR23 might explain some of the pathological and physiological roles of LPA in ovary. It remains to be determined whether the expression of p2y$_9$/GPR23 is modulated in ovarian cancer cells. Although the EST cDNA encoding p2y$_9$/GPR23 was originally isolated from human brain (25, 26), high expression of p2y$_9$/GPR23 was not detected in brain in our study. It is possible that specific types of cells in re-

stricted areas express $p2y_9$/GPR23, which will be examined by *in situ* hybridization in the near future.

Interestingly, $p2y_9$/GPR23 shares only 20–24% amino acid identities with Edg-2/LPA_1, Edg-4/LPA_2, and Edg-7/LPA_3. Phylogenetic analysis also shows that $p2y_9$/GPR23 is far distant from the Edg family (Fig. 1). These facts suggest that $p2y_9$/GPR23 has evolved from ancestor sequences that are different from those of the Edg family. There are several examples of structurally unrelated receptors recognizing the same ligand. Prostaglandin D_2 binds to DP and CRTH2 (38) and histamine has four structurally distant receptors, H_1–H_4 (39). In addition, some neurotransmitters and nucleotides have both metabotropic (G protein-coupled) and ionotropic (ion channel) receptors. These examples show a limitation of the ligand search strategy utilizing a structural similarity of receptor.

As described above, there are some reports implying the existence of additional receptors for LPA. It is possible that LPA-induced responses in embryonic fibroblast cells of Edg-2/$LPA_1^{(-/-)}$ Edg-4/$LPA_2^{(-/-)}$ double knockout mice (10) might be mediated by $p2y_9$/GPR23, although we do not have any direct evidence. However, a mitogenic response to LPA in RH7777 cells (12) might be due to the activity of intracellular receptors (40), rather than G protein-coupled receptor, because mock-transfected RH7777 cells exhibited no significant binding to [^{3}H]LPA (Fig. 2*A*). As to the putative LPA receptor in platelets (11, 13), there may be a receptor other than $p2y_9$/GPR23, because the ligand preference of platelets to 1-alkyl-LPAs is not consistent with that of $p2y_9$/GPR23. Existence of further unidentified LPA receptors is, therefore, expected.

In conclusion, we report here the identification of $p2y_9$/GPR23 as a novel fourth LPA receptor (LPA_4). Cells expressing $p2y_9$/GPR23 displayed intracellular Ca^{2+} mobilization, cAMP accumulation, and luciferase activation. The K_d value of $p2y_9$/GPR23 (45 nM) was equivalent to those of Edg-4/LPA_2 (73.6 nM) and Edg-7/LPA_3 (206 nM) (9). Although $p2y_9$/GPR23 mRNA was significantly detected in ovary, its biological functions *in vivo* remain to be determined. Nevertheless, the present findings introduce a further complexity for LPA and its receptors. In addition, our study shows a limitation of the "de-orphaning" strategy based on the receptor structure.

Acknowledgments—We thank Dr. T. Yokomizo and H. Hagiya (The University of Tokyo) for vital discussions and critical suggestions. We are also grateful to Dr. J. Miyazaki (Osaka University, Japan) for supplying pCXN2, and H. Shindou for expert technique of binding assay.

REFERENCES

1. Tokumura, A. (1995) *Prog. Lipid Res.* **34,** 151–184
2. Contos, J. J., Ishii, I., and Chun, J. (2000) *Mol. Pharmacol.* **58,** 1188–1196
3. Fukushima, N., Ishii, I., Contos, J. J., Weiner, J. A., and Chun, J. (2001) *Annu. Rev. Pharmacol. Toxicol.* **41,** 507–534
4. Tigyi, G., and Miledi, R. (1992) *J. Biol. Chem.* **267,** 21360–21367
5. Aoki, J., Taira, A., Takanezawa, Y., Kishi, Y., Hama, K., Kishimoto, T., Mizuno, K., Saku, K., Taguchi, R., and Arai, H. (2002) *J. Biol. Chem.* **277,** 48737–48744
6. Pages, C., Simon, M. F., Valet, P., and Saulnier-Blache, J. S. (2001) *Prostaglandins Other Lipid Mediat.* **64,** 1–10
7. Hecht, J. H., Weiner, J. A., Post, S. R., and Chun, J. (1996) *J. Cell Biol.* **135,** 1071–1083
8. An, S., Bleu, T., Hallmark, O. G., and Goetzl, E. J. (1998) *J. Biol. Chem.* **273,** 7906–7910
9. Bandoh, K., Aoki, J., Hosono, H., Kobayashi, S., Kobayashi, T., Murakami-Murofushi, K., Tsujimoto, M., Arai, H., and Inoue, K. (1999) *J. Biol. Chem.* **274,** 27776–27785
10. Contos, J. J., Ishii, I., Fukushima, N., Kingsbury, M. A., Ye, X., Kawamura, S., Brown, J. H., and Chun, J. (2002) *Mol. Cell. Biol.* **22,** 6921–6929
11. Gueguen, G., Gaige, B., Grevy, J. M., Rogalle, P., Bellan, J., Wilson, M., Klaebe, A., Pont, F., Simon, M. F., and Chap, H. (1999) *Biochemistry* **38,** 8440–8450
12. Hooks, S. B., Santos, W. L., Im, D. S., Heise, C. E., Macdonald, T. L., and Lynch, K. R. (2001) *J. Biol. Chem.* **276,** 4611–4621
13. Tokumura, A., Sinomiya, J., Kishimoto, S., Tanaka, T., Kogure, K., Sugiura, T., Satouchi, K., Waku, K., and Fukuzawa, K. (2002) *Biochem. J.* **365,** 617–628
14. Nakamura, M., Honda, Z., Izumi, T., Sakanaka, C., Mutoh, H., Minami, M., Bito, H., Seyama, Y., Matsumoto, T., Noma, M., and Shimizu, T. (1991) *J. Biol. Chem.* **266,** 20400–20405
15. Niwa, H., Yamamura, K., and Miyazaki, J. (1991) *Gene (Amst.)* **108,** 193–199
16. Ogasawara, H., Ishii, S., Yokomizo, T., Kakinuma, T., Komine, M., Tamaki, K., Shimizu, T., and Izumi, T. (2002) *J. Biol. Chem.* **277,** 18763–18768
17. Boeynaems, J. M., Communi, D., Savi, P., and Herbert, J. M. (2000) *Trends Pharmacol. Sci.* **21,** 1–3
18. Hla, T., Lee, M. J., Ancellin, N., Paik, J. H., and Kluk, M. J. (2001) *Science* **294,** 1875–1878
19. Fukushima, N., Kimura, Y., and Chun, J. (1998) *Proc. Natl. Acad. Sci. U. S. A.* **95,** 6151–6156
20. Ogura, M., Morishima, Y., Ohno, R., Kato, Y., Hirabayashi, N., Nagura, H., and Saito, H. (1985) *Blood* **66,** 1384–1392
21. Baker, D. L., Desiderio, D. M., Miller, D. D., Tolley, B., and Tigyi, G. J. (2001) *Anal. Biochem.* **292,** 287–295
22. Sugiura, T., Nakane, S., Kishimoto, S., Waku, K., Yoshioka, Y., Tokumura, A., and Hanahan, D. J. (1999) *Biochim. Biophys. Acta* **1440,** 194–204
23. Liliom, K., Guan, Z., Tseng, J. L., Desiderio, D. M., Tigyi, G., and Watsky, M. A. (1998) *Am. J. Physiol.* **274,** C1065–C1074
24. Xu, Y., Gaudette, D. C., Boynton, J. D., Frankel, A., Fang, X. J., Sharma, A., Hurteau, J., Casey, G., Goodbody, A., and Mellors, A. (1995) *Clin. Cancer Res.* **1,** 1223–1232
25. O'Dowd, B. F., Nguyen, T., Jung, B. P., Marchese, A., Cheng, R., Heng, H. H., Kolakowski, L. F., Jr., Lynch, K. R., and George, S. R. (1997) *Gene (Amst.)* **187,** 75–81
26. Janssens, R., Boeynaems, J. M., Godart, M., and Communi, D. (1997) *Biochem. Biophys. Res. Commun.* **236,** 106–112
27. An, S., Bleu, T., Zheng, Y., and Goetzl, E. J. (1998) *Mol. Pharmacol.* **54,** 881–888
28. Bandoh, K., Aoki, J., Taira, A., Tsujimoto, M., Arai, H., and Inoue, K. (2000) *FEBS Lett.* **478,** 159–165
29. Im, D. S., Heise, C. E., Harding, M. A., George, S. R., O'Dowd, B. F., Theodorescu, D., and Lynch, K. R. (2000) *Mol. Pharmacol.* **57,** 753–759
30. Carruthers, A. M., Warner, A. J., Michel, A. D., Feniuk, W., and Humphrey, P. P. (1999) *Br. J. Pharmacol.* **126,** 1221–1229
31. Michal, P., Lysikova, M., and Tucek, S. (2001) *Br. J. Pharmacol.* **132,** 1217–1228
32. Sunahara, R. K., Dessauer, C. W., and Gilman, A. G. (1996) *Annu. Rev. Pharmacol. Toxicol.* **36,** 461–480
33. Varga, E. V., Stropova, D., Rubenzik, M., Wang, M., Landsman, R. S., Roeske, W. R., and Yamamura, H. I. (1998) *Eur. J. Pharmacol.* **348,** R1–R2
34. Fang, X., Gaudette, D., Furui, T., Mao, M., Estrella, V., Eder, A., Pustilnik, T., Sasagawa, T., Lapushin, R., Yu, S., Jaffe, R. B., Wiener, J. R., Erickson, J. R., and Mills, G. B. (2000) *Ann. N. Y. Acad. Sci.* **905,** 188–208
35. Goetzl, E. J., Dolezalova, H., Kong, Y., and Zeng, L. (1999) *Cancer Res.* **59,** 4732–4737
36. Jaspard, B., Collet, X., Barbaras, R., Manent, J., Vieu, C., Parinaud, J., Chap, H., and Perret, B. (1996) *Biochemistry* **35,** 1352–1357
37. Tokumura, A. (2002) *Biochim. Biophys. Acta* **1582,** 18–25
38. Hirai, H., Tanaka, K., Yoshie, O., Ogawa, K., Kenmotsu, K., Takamori, Y., Ichimasa, M., Sugamura, K., Nakamura, M., Takano, S., and Nagata, K. (2001) *J. Exp. Med.* **193,** 255–261
39. Schneider, E., Rolli-Derkinderen, M., Arock, M., and Dy, M. (2002) *Trends Immunol.* **23,** 255–263
40. McIntyre, T. M., Pontsler, A. V., Silva, A. R., St. Hilaire, A., Xu, Y., Hinshaw, J. C., Zimmerman, G. A., Hama, K., Aoki, J., Arai, H., and Prestwich, G. D. (2003) *Proc. Natl. Acad. Sci. U. S. A.* **100,** 131–136

Improved Host Defense against Pneumococcal Pneumonia in Platelet-Activating Factor Receptor–Deficient Mice

Anita W. Rijneveld,[1,2] Sebastiaan Weijer,[1,2] Sandrine Florquin,[3] Peter Speelman,[2,4] Takao Shimizu,[5] Satosh Ishii,[5] and Tom van der Poll[1,4]

[1]Laboratory of Experimental Internal Medicine and Departments of [2]Internal Medicine, [3]Pathology, and [4]Infectious Diseases, Tropical Medicine, and AIDS, Academic Medical Center, University of Amsterdam, Amsterdam, The Netherlands; [5]Department of Biochemistry and Molecular Biology, Faculty of Medicine, University of Tokyo, and CREST of Japan Science and Technology Corporation, Tokyo, Japan

Platelet-activating factor (PAF) is a phospholipid with proinflammatory properties that binds to a specific receptor (PAF receptor [PAFR]) that is expressed on many different cell types. PAFR is able to bind phosphorylcholine, which is present in both PAF and the pneumococcal cell wall. Activation of respiratory epithelial cells in vitro results in up-regulation of PAFR, which, in turn, facilitates invasion of *Streptococcus pneumoniae*. To determine the role of PAFR in host defense against pneumococcal pneumonia, PAFR-deficient ($PAFR^{-/-}$) and wild-type *(wt)* mice were inoculated intranasally with *S. pneumoniae*. $PAFR^{-/-}$ mice were relatively resistant to pneumococcal pneumonia, as indicated by delayed and reduced mortality, diminished outgrowth of pneumococci in lungs, and reduced dissemination of the infection (all $P < .05$, vs. *wt* mice). $PAFR^{-/-}$ mice also had less pulmonary inflammation. These data provide evidence that PAFR is used by *S. pneumoniae* to induce lethal pneumonia.

Platelet-activating factor (PAF) is a glycerophospholipid produced mainly by platelets, endothelial cells, macrophages, and neutrophils that plays an important role in the orchestration of different inflammatory reactions [1–3]. The biological activity of PAF is mediated through a specific G-protein–linked receptor (PAF receptor [PAFR]) that is expressed on different cell types, including neutrophils, monocytes, macrophages, and epithelial cells. Via PAFR, PAF exerts several immunomodulatory actions involved in host defense against bacterial infections, including stimulation of migration and degranulation of granulocytes, monocytes, and macrophages and the release of cytokines and toxic oxygen metabolites [1–3].

PAFR has been thought to play a crucial role in the pathogenesis of pneumococcal disease [4]. The biological activity of PAF is mainly determined by phosphorylcholine (PC), which binds specifically to PAFR [1–3]; PC is also a prominent part of the cell wall of *Streptococcus pneumoniae* [5]. Activation of endothelial or epithelial cells results in up-regulation of PAFR at their surface, which, in turn, facilitates invasion by *S. pneumoniae* via an interaction between PAFR and the PC component of the pneumococcal cell wall [6–8]. The relevance in vivo of the interaction between pneumococcal PC and PAFR is supported by several findings. First, administration of either a PAFR antagonist or an anti-PC antibody reduced leukocytosis and protein concentrations in the cerebrospinal fluid of rabbits injected intracisternally with *S. pneumoniae* [9]. Second, administration of a PAFR antagonist also reduced the recruitment of leukocytes and the increase in protein concentrations in bronchoalveolar lavage (BAL) fluid (BALF) of rabbits challenged intratracheally (int) with killed *S. pneumoniae* [9]. Third, the combination

Received 19 February 2003; accepted 29 June 2003; electronically published 30 January 2004.

Financial support: Dutch Association for Scientific Research (grants to A.W.R. and S.W.); Ministry of Health, Labour, and Welfare, Japan (grants-in-aid for comprehensive research on aging and health and for research on allergic disease and immunology to S.I.).

Reprints or correspondence: Dr. Anita W. Rijneveld, Academic Medical Center, University of Amsterdam, F4-105, Meibergdreef 9, 1105 AZ Amsterdam, The Netherlands (a.w.rijneveld@amc.uva.nl).

The Journal of Infectious Diseases 2004;189:711–6

0022-1899/2004/18904-0020$15.00

of int administration of live *S. pneumoniae* and a PAFR antagonist to rabbits resulted in reduced bacteria loads in BALF obtained up to 48 h after inoculation, compared with BALF from animals given pneumococci only [6]. A recent study, however, reported enhanced bacterial outgrowth after intravenous treatment with a PAFR antagonist in a mouse model of pneumococcal pneumonia [10].

The objective of the present study was to obtain more insight into the role of PAFR in the pathogenesis of pneumococcal pneumonia. For this purpose, we compared host responses in PAFR-deficient ($PAFR^{-/-}$) and normal wild-type *(wt)* mice after intranasal (inl) inoculation with live *S. pneumoniae.*

MATERIALS AND METHODS

Animals. $PAFR^{-/-}$ mice were generated in Japan, as described elsewhere [11], and were shipped to the animal facility of the Academic Medical Center in Amsterdam in 1999 (i.e., 3 years before the experiments were conducted). Hence, all $PAFR^{-/-}$ mice used in the present study were born in Amsterdam. $PAFR^{-/-}$ mice were backcrossed 7 times to a C57BL/6 background, making them 99.6% pure C57BL/6. *wt* C57BL/6 mice were obtained from Harlan Sprague Dawley. Both $PAFR^{-/-}$ and *wt* mice were specific pathogen free. All experiments were conducted with 10–12-week-old male mice. Fighting between mice did not occur during the studies described. All experiments were approved by the Institutional Animal Care and Use Committee of the Academic Medical Center.

Induction of pneumonia. Pneumococcal pneumonia was induced as described elsewhere [12, 13]. In brief, *S. pneumoniae* serotype 3 (ATCC 6303) were grown in Todd-Hewitt broth (Difco) for 6 h to mid-logarithmic phase at 37°C, harvested by centrifugation at 1500 *g* for 15 min, and washed twice in sterile isotonic saline. Bacteria were then resuspended in sterile isotonic saline at a concentration of $\sim 1 \times 10^7$ cfu/mL, as determined by plating serial 10-fold dilutions on sheep's blood agar plates. Mice were lightly anesthesized by inhalation of isoflurane (Abott), and 50 μL of bacterial suspension was inoculated inl, corresponding with 5×10^5 cfu of *S. pneumoniae.*

Preparation of lung homogenates. At 24 or 48 h after inoculation, mice were anesthetized by intraperitoneal injection with Hypnorm (Janssen Pharmaceutica) and midazolam (Roche), and blood was obtained from the inferior caval vene. Whole lungs were harvested and homogenized at 4°C in 5 volumes of sterile isotonic saline by use of a tissue homogenizer (Biospect Products), which was carefully cleaned and disinfected with 70% ethanol after each homogenization. Serial 10-fold dilutions in sterile saline were made from these lung homogenates and from blood, and 50-μL volumes were plated onto sheep's blood agar plates and incubated at 37°C. Colony-forming units were counted after 16 h. For cytokine measurements, lung homogenates were lysed in lysis buffer (300 mmol/L NaCl, 15 mmol/L Tris, 2 mmol/L MgCl, 2 mmol/L Triton X-100, and 20 ng/mL pepstatin A, leupeptin, and aprotinin [pH 7.4]) and spun at 1500 *g* at 4°C for 15 min; the supernatant was frozen at −20°C until cytokine measurement.

BAL. The trachea was exposed through a midline incision and was cannulated with a sterile 22-gauge Abbocath-T catheter (Abbott). BAL was performed by instilling two 0.5-mL aliquots of sterile isotonic saline; 0.9–1 mL of BALF was retrieved from each mouse, and total cell numbers were counted from each sample in a hemocytometer (Emergo). BALF differential cell counts were determined on cytospin preparations stained with modified Giemsa stain (Diff-Quick).

Histologic examination. After lungs were fixed in 10% formaline and embedded in paraffin for 24 h, 4-μm–thick sections were stained with hematoxylin-eosin. All slides were coded and scored by a pathologist who did not know the genotype of the mice.

Assays. Levels of the following cytokines and chemokines were measured by use of commercially available ELISAs, in accordance with the manufacturers' recommendations: tumor necrosis factor (TNF)–α and interleukin (IL)–6 (Pharmingen) and IL-1β, macrophage inflammatory protein (MIP)–2, and KC (R&D systems). Limits of detection were 150 pg/mL for TNF-α and IL-1β, 75 pg/mL for IL-6, 47 pg/mL for MIP-2, and 12 pg/mL for KC. Protein concentrations were measured in BALF by use of a commercially available assay (Micro Bicinchoninic Acid Protein Assay; Pierce Biotechnology), according to the recommendations of the manufacturer.

Statistical analysis. Data are shown as means ± SEM, unless otherwise indicated. Comparisons between groups were conducted by use of the Mann-Whitney *U* test. Survival curves were compared by log-rank test. $P < .05$ was considered to be statistically significant.

RESULTS

Protection against pneumococcal pneumonia in $PAFR^{-/-}$ mice. To investigate the involvement of PAFR in the outcome of pneumococcal pneumonia, $PAFR^{-/-}$ and *wt* mice were infected inl with 5×10^5 cfu of *S. pneumoniae* and monitored for 10 days. All *wt* mice died within 85 h after induction of pneumonia. Mortality was delayed and reduced among $PAFR^{-/-}$ mice; 21% survived until the end of the 10-day observation period ($P < .0001$, *wt* vs. $PAFR^{-/-}$ mice; figure 1).

Reduced outgrowth of pneumococci in $PAFR^{-/-}$ mice. To obtain insight into the role of PAFR in early antibacterial defense during pneumococcal pneumonia, we assessed the number of viable bacteria in the lungs 24 and 42 h after inoculation (i.e., at time points before the occurrence of the first deaths). At both time points, the numbers of colony-forming units recovered from

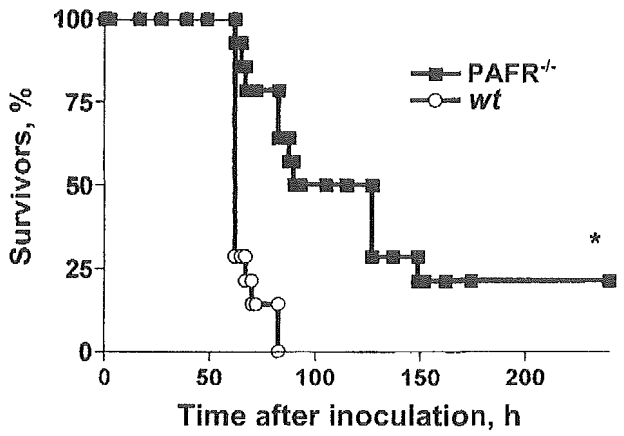

Figure 1. Enhanced survival in platelet-activating factor receptor–deficient (PAFR$^{-/-}$) mice. Survival after intranasal inoculation with *Streptococcus pneumoniae* in wild-type *(wt)* (○) and PAFR$^{-/-}$ (■) mice was assessed twice daily for 10 days (n = 14 mice/group). *P < .05, vs. *wt* mice.

the lungs of PAFR$^{-/-}$ mice were significantly lower than those recovered from *wt* mice (P < .05; figure 2). At 24 h after inoculation, blood cultures were positive for 71% of the *wt* mice and for 14% of the PAFR$^{-/-}$ mice (P = .03). At 42 h after inoculation, blood cultures were positive for 83% of the *wt* mice and for 50% of the PAFR$^{-/-}$ mice (P, not significant).

Unaltered neutrophil numbers and protein concentrations in BALF of PAFR$^{-/-}$ mice. Neutrophils play a prominent role in host defense against bacterial pneumonia [14, 15]. Because inhibition of PAFR function has been shown to reduce leukocyte influx into the lungs in response to intrapulmonary delivery of killed pneumococci [9], we assessed the number of neutrophils recruited to the alveoli. At 42 h after inoculation, no difference was seen in the number of neutrophils in BALF from *wt* and PAFR$^{-/-}$ mice (figure 3). Moreover, protein concentrations measured in BALF at this time point did not differ between PAFR$^{-/-}$ and *wt* mice (234.3 ± 42.8 and 298.3 ± 68.4 μg/mL, respectively).

Histologic analysis. At 42 h after inoculation, lungs of *wt* mice displayed heavy inflammatory infiltrates characterized by endothelialitis, peribronchial inflammation, and pleuritis. Lung inflammation was clearly less pronounced in PAFR$^{-/-}$ mice (figure 4).

Lung cytokine and chemokine concentrations. Cytokines and chemokines are pivotal mediators of an adequate host response to bacterial infection of the respiratory tract [14, 16]. Therefore, we investigated whether the improved outcome of PAFR$^{-/-}$ mice was associated with a favorable shift in cytokine or chemokine production by measuring the concentrations of TNF-α, IL-1β, IL-6, KC, and MIP-2 in lung homogenates. However, at 24 h after the induction of pneumonia, the pulmonary levels of these protective mediators were lower in PAFR$^{-/-}$ mice than in *wt* mice (all P < .05), whereas, at 42 h, all levels were similar in both mouse strains (table 1).

DISCUSSION

S. pneumoniae is the most frequently isolated pathogen in community-acquired pneumonia [17]. In the United States alone, >500,000 cases of pneumococcal pneumonia are reported each year, with a fatality rate of 5%–7%. In recent sepsis trials, *S. pneumoniae* emerged as an important causative pathogen, especially in the context of pneumonia [18]. In the United States, the mortality rate of 40,000 deaths/year caused by *S. pneumoniae* is higher than that caused by any other bacterial pathogen [19]. Because infections caused by *S. pneumoniae* are increasingly difficult to treat as a result of the emergence of antibiotic-resistant strains, it is clear that respiratory-tract infection by *S. pneumoniae* represents a major health care problem. Fundamental research has elucidated an important mechanism by which the pneumococcus interacts with cells lining the respiratory tract to cause tissue invasion. In particular, the PC component that prominently features in the pneumococcal cell wall specifically binds to PAFR expressed on human respiratory ep-

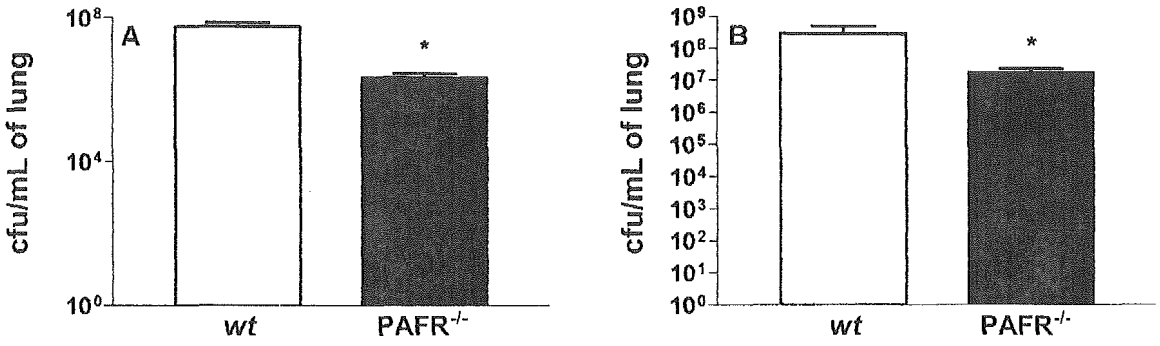

Figure 2. Decreased nos. *Streptococcus pneumoniae* organisms in lungs of platelet-activating factor receptor–deficient (PAFR$^{-/-}$) mice. Pneumococci in lungs of wild-type *(wt) (white bars)* and PAFR$^{-/-}$ *(black bars)* mice were measured 24 *(A)* and 42 *(B)* h after inoculation with *S. pneumoniae*. Data are mean ± SEM (n = 7 mice/group/time point). *P < .05, vs. *wt* mice.

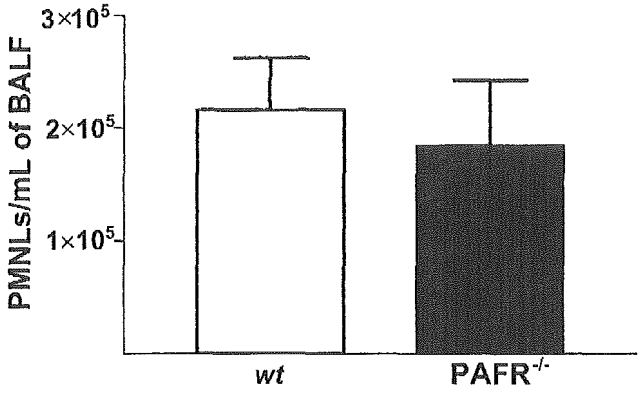

Figure 3. Mean ± SEM granulocyte influx in bronchoalveolar lavage fluid (BALF) 48 h after intranasal inoculation of *Streptococcus pneumoniae* in wild-type *(wt)* and platelet-activating factor receptor–deficient ($PAFR^{-/-}$) mice (n = 8 mice/group). PAFR deficiency does not influence recruitment of polymorphonuclear leukocytes (PMNLs) into alveoli during pneumococcal pneumonia. $^*P < .05$, vs. *wt* mice.

ithelial cells, which facilitates bacterial entry into these cells [6]. In addition, the capacity of pneumococci to transcytose to the basal surface of rat and human endothelial cells is dependent on PAFR [7]. Although, to our knowledge, an interaction between pneumococci and the murine PAFR has not been formally demonstrated, here we provide compelling evidence that this mechanism is important for the virulence of pneumococci during murine respiratory tract infection in vivo. Using $PAFR^{-/-}$ mice, we have demonstrated that PAFR is used by *S. pneumoniae* to induce lethal pneumonia, as reflected by greatly reduced mortality, attenuated bacterial outgrowth in the lungs, and diminished dissemination of the infection in $PAFR^{-/-}$ mice.

The favorable outcome of $PAFR^{-/-}$ mice can not be explained by an enhanced innate immune response to *S. pneumoniae.* Indeed, even the local levels of protective cytokines and chemokines were lower in $PAFR^{-/-}$ mice early after the inoculation, suggesting that the initiation of the production of these mediators depends, at least in part, on the early interaction between pneumococci and PAFR. Alternatively, the absence of PAF signaling itself may have contributed to this finding, because inhibition of PAF has been found to attenuate the production of cytokines, especially TNF-α, induced by lipopolysaccharide (LPS) [1–3]. Similarly, the attenuated inflammatory response in lung tissue of $PAFR^{-/-}$ mice can be explained by either the absence of an interaction between pneumococcal PC and PAFR, the absence of endogenous PAF activity, or the presence of lower bacteria loads in the lungs of $PAFR^{-/-}$ mice, providing a less potent proinflammatory stimulus to the direct environment. Of note, neutrophil influx and protein concentrations in the BALF were similar in $PAFR^{-/-}$ and *wt* mice, which contradicts the results of earlier investigations, demonstrating that local administration of a PAFR antagonist diminished leukocytosis and increased protein concentrations in the cerebrospinal fluid and BALF of rabbits given *S. pneumoniae* intracisternally or int, respectively [9].

To our knowledge, 2 earlier studies investigated the effect of PAFR antagonists on the outgrowth of pneumococci in models of pneumonia. In the first study [6], a PAFR antagonist administered int together with *S. pneumoniae* reduced the number of colony-forming units recovered from BALF obtained up to 48 h after inoculation in rabbits, compared with BALF from rabbits administered bacteria only. In the second study [10], mice that received another PAFR antagonist intravenously had higher bacteria loads than did control mice. The 2 types of data indicate differences that remain to be explained, although spe-

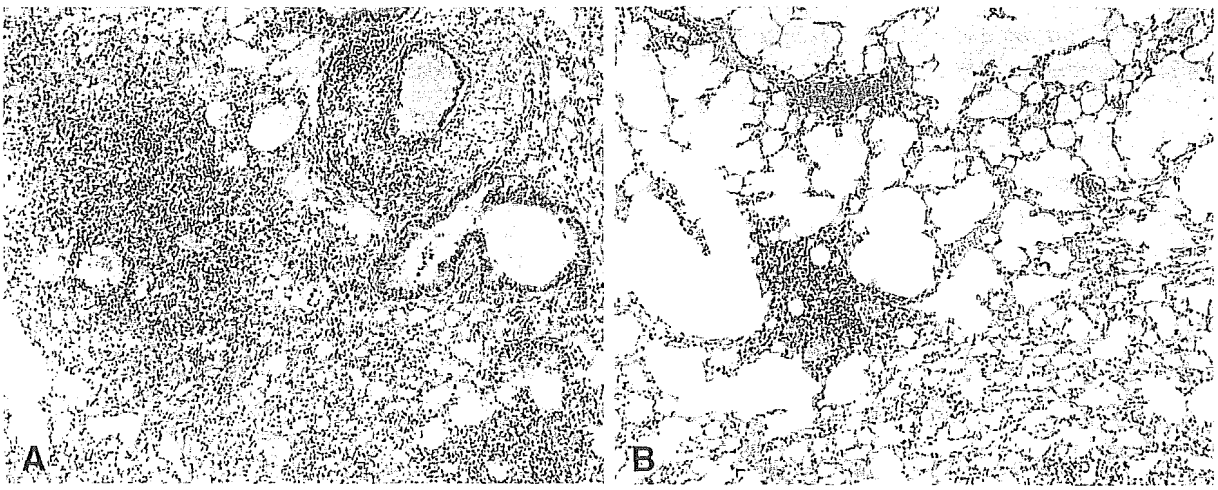

Figure 4. Histopathologic analysis of lungs, 42 h after inoculation with *Streptococcus pneumoniae,* shows heavy inflammatory infiltrates characterized by endothelialitis, peribronchial inflammation, and pleuritis. Lung inflammation was clearly less pronounced in platelet-activating factor receptor–deficient mice *(B)* than in wild-type mice *(A).* Representative slides are shown (hematoxylin-eosin staining; original magnification, ×33).

Table 1. Cytokine and chemokine concentrations in lung homogenates of wild-type *(wt)* and platelet-activating factor receptor–deficient ($PAFR^{-/-}$) mice inoculated with *Streptococcus pneumoniae*.

Cytokine/ chemokine	24 h after inoculation		42 h after inoculation	
	wt	$PAFR^{-/-a}$	*wt*	$PAFR^{-/-}$
TNF-α	2.1 ± 0.4	0.9 ± 0.2	1.8 ± 0.3	2.7 ± 1.1
IL-1β	8 ± 0.8	3.3 ± 1.1	4.3 ± 0.8	6.4 ± 2.1
IL-6	5.3 ± 0.6	1.7 ± 0.7	4.3 ± 0.7	3.6 ± 1.2
KC	8.8 ± 0.5	5.8 ± 0.6	9.6 ± 0.9	7.8 ± 1.6
MIP-2	7.0 ± 1.5	4.3 ± 0.6	29.4 ± 10.6	8.1 ± 1.8

NOTE. Data are mean ± SEM nanograms of each cytokine or chemokine per milliliter of lung homogenate (n = 8 mice/group). IL, interleukin; MIP, macrophage inflammatory protein; TNF-α, tumor necrosis factor–α.

[a] $P < .05$, vs. *wt* mice.

cific properties of the PAFR antagonist may have played a role. Nonetheless, the present data obtained with $PAFR^{-/-}$ mice, together with earlier data [6, 9], are consistent with the hypothesis that PAFR is used by *S. pneumoniae* in vivo to cause severe pneumonia.

PAF functions as a proinflammatory mediator in models of severe bacterial infection. Indeed, high PAF levels were detected in the lungs of rats after systemic injection of LPS [20] and in the BALF of patients with sepsis [21]. Inhalation of aerosolized PAF provoked inflammatory cell influx in the interstitium and alveoli [22, 23]. Finally, pretreatment with PAFR antagonists strongly diminished the pulmonary changes elicited by systemic or intrapulmonary administration of LPS, including increased pulmonary vascular leak and edema [24–27]. Together, these data suggest that PAF promotes inflammatory responses to bacteria, especially in the lung. A proinflammatory role for PAF in the pulmonary compartment is further supported by recent findings in $PAFR^{-/-}$ mice, revealing strongly reduced lung injury and respiratory failure induced by aspiration of acid [28]. Theoretically, these proinflammatory properties would make PAF a potentially protective mediator during pneumonia [14, 16]. Such a protective role of PAF in host defense against respiratory tract infection indeed was found in a model of pneumonia caused by *Klebsiella pneumoniae*, a bacterium that does not express PC, using the same type of $PAFR^{-/-}$ mice that were used in the present study [29]. The present investigation clearly establishes that the absence of PAFR overshadows this potential PAF-mediated increase in antibacterial defense, most likely through a function that is unrelated to its interaction with PAF (i.e., through its interaction with pneumococcal PC). These data may also apply to other pathogens that express PC, although this needs to be investigated in future studies.

It has been shown that *S. pneumoniae* needs PAFR to enter epithelial cells. Indeed, our study confirms this by showing that $PAFR^{-/-}$ mice are less likely to develop invasive disease and have improved host defense during pneumococcal infection. Thus, PAFR antagonism appears to be protective. However, the blockage of the proinflammatory properties of PAF by this strategy might be detrimental in acute inflammation.

References

1. Kuijpers TW, van der Poll T. The role of PAF in endotoxin-related disease. In: Brade H, Opal SM, Vogel SN, Morrison DC, eds. Endotoxin in health and disease. New York: Marcel Dekker, 1999:449–62.
2. Ishii S, Shimizu T. Platelet-activating factor (PAF) receptor and genetically engineered PAF receptor mutant mice. Prog Lipid Res 2000;39: 41–82.
3. Prescott SM, Zimmerman GA, Stafforini DM, McIntyre TM. Platelet-activating factor and related lipid mediators. Annu Rev Biochem 2000; 69:419–45.
4. McCullers JA, Tuomanen EI. Molecular pathogenesis of pneumococcal pneumonia. Front Biosci 2001;6:D877–89.
5. Fischer W. Phosphocholine of pneumococcal teichoic acids: role in bacterial physiology and pneumococcal infection. Res Microbiol 2000; 151:421–7.
6. Cundell DR, Gerard NP, Gerard C, Idanpaan-Heikkila I, Tuomanen EI. *Streptococcus pneumoniae* anchor to activated human cells by the receptor for platelet-activating factor. Nature 1995;377:435–8.
7. Ring A, Weiser JN, Tuomanen EI. Pneumococcal trafficking across the blood-brain barrier: molecular analysis of a novel bidirectional pathway. J Clin Invest 1998; 102:347–60.
8. Ishizuka S, Yamaya M, Suzuki T, et al. Acid exposure stimulates the adherence of *Streptococcus pneumoniae* to cultured human airway epithelial cells: effects on platelet-activating factor receptor expression. Am J Respir Cell Mol Biol 2001;24:459–68.
9. Cabellos C, MacIntyre DE, Forrest M, Burroughs M, Prasad S, Tuomanen E. Differing roles for platelet-activating factor during inflammation of the lung and subarachnoid space: the special case of *Streptococcus pneumoniae*. J Clin Invest 1992; 90:612–8.
10. McCullers JA, Rehg JE. Lethal synergism between influenza virus and *Streptococcus pneumoniae:* characterization of a mouse model and the role of platelet-activating factor receptor. J Infect Dis 2002; 186:341–50.
11. Ishii S, Kuwaki T, Nagase T, et al. Impaired anaphylactic responses with intact sensitivity to endotoxin in mice lacking a platelet-activating factor receptor. J Exp Med 1998; 187:1779–88.
12. Rijneveld AW, Florquin S, Branger J, Speelman P, Van Deventer SJ, van der Poll T. TNF-α compensates for the impaired host defense of IL-1 type I receptor–deficient mice during pneumococcal pneumonia. J Immunol 2001; 167:5240–6.
13. van der Poll T, Keogh CV, Buurman WA, Lowry SF. Passive immunization against tumor necrosis factor–α impairs host defense during pneumococcal pneumonia in mice. Am J Respir Crit Care Med 1997; 155:603–8.
14. Moore TA, Standiford TJ. Cytokine immunotherapy during bacterial pneumonia: from benchtop to bedside. Semin Respir Infect 2001; 16: 27–37.
15. Zhang P, Summer WR, Bagby GJ, Nelson S. Innate immunity and pulmonary host defense. Immunol Rev 2000; 173:39–51.
16. Schultz M, Rijneveld A, van der Poll T. Cytokines and innate immunity against bacterial respiratory pathogens. In: Pandalai SG, ed. Recent research developments in immunology, part I. Vol 3. Kerala, India: Research Signpost, 2001:1–13.
17. Bartlett JG, Dowell SF, Mandell LA, File TM Jr, Musher DM, Fine MJ. Practice guidelines for the management of community-acquired pneumonia in adults. Infectious Diseases Society of America. Clin Infect Dis 2000; 31:347–82.
18. Bernard GR, Vincent JL, Laterre PF, et al. Efficacy and safety of recombinant human activated protein C for severe sepsis. N Engl J Med 2001; 344:699–709.

19. Jedrzejas MJ. Pneumococcal virulence factors: structure and function. Microbiol Mol Biol Rev **2001**;65:187–207.
20. Chang SW, Feddersen CO, Henson PM, Voelkel NF. Platelet-activating factor mediates hemodynamic changes and lung injury in endotoxin-treated rats. J Clin Invest **1987**;79:1498–509.
21. Sorensen J, Kald B, Tagesson C, Lindahl M. Platelet-activating factor and phospholipase A2 in patients with septic shock and trauma. Intensive Care Med **1994**;20:555–61.
22. O'Connor BJ, Uden S, Carty TJ, Eskra JD, Barnes PJ, Chung KF. Inhibitory effect of UK,74505, a potent and specific oral platelet activating factor (PAF) receptor antagonist, on airway and systemic responses to inhaled PAF in humans. Am J Respir Crit Care Med **1994**; 150:35–40.
23. Rodriguez-Roisin R, Felez MA, Chung KF, et al. Platelet-activating factor causes ventilation-perfusion mismatch in humans. J Clin Invest **1994**;93:188–94.
24. Siebeck M, Weipert J, Keser C, et al. A triazolodiazepine platelet activating factor receptor antagonist (WEB 2086) reduces pulmonary dysfunction during endotoxin shock in swine. J Trauma **1991**;31:942–9.
25. Dobrowsky RT, Voyksner RD, Olson NC. Effect of SRI 63–675 on hemodynamics and blood PAF levels during porcine endotoxemia. Am J Physiol **1991**;260:H1455–65.
26. Miotla JM, Jeffery PK, Hellewell PG. Platelet-activating factor plays a pivotal role in the induction of experimental lung injury. Am J Respir Cell Mol Biol **1998**;18:197–204.
27. Rylander R, Beijer L, Lantz RC, Burrell R, Sedivy P. Modulation of pulmonary inflammation after endotoxin inhalation with a platelet-activating factor antagonist (48740 RP). Int Arch Allergy Appl Immunol **1988**;86:303–7.
28. Nagase T, Ishii S, Kume K, et al. Platelet-activating factor mediates acid-induced lung injury in genetically engineered mice. J Clin Invest **1999**; 104:1071–6.
29. Soares AC, Pinho VS, Souza DG, et al. Role of the platelet-activating factor (PAF) receptor during pulmonary infection with gram negative bacteria. Br J Pharmacol **2002**;137:621–8.

Platelet-Activating Factor Receptor Develops Airway Hyperresponsiveness Independently of Airway Inflammation in a Murine Asthma Model[1]

Satoshi Ishii,[2*§] Takahide Nagase,[†] Hideo Shindou,[*§] Hajime Takizawa,[†] Yasuyoshi Ouchi,[‡] and Takao Shimizu[*§]

Lipid mediators play an important role in modulating inflammatory responses. Platelet-activating factor (PAF) is a potent proinflammatory phospholipid with eosinophil chemotactic activity in vitro and in vivo. We show in this study that mice deficient in PAF receptor exhibited significantly reduced airway hyperresponsiveness to muscarinic cholinergic stimulation in an asthma model. However, PAF receptor-deficient mice developed an eosinophilic inflammatory response at a comparable level to that of wild-type mice. These results indicate an important role for PAF receptor, downstream of the eosinophilic inflammatory cascade, in regulating airway responsiveness after sensitization and aeroallergen challenge. *The Journal of Immunology,* **2004, 172: 7095–7102.**

Bronchial asthma is a complex disease of the lung characterized by reversible airway obstruction, chronic airway inflammation, and airway hyperresponsiveness (AHR)[3] to nonspecific stimuli. The progression of airway inflammation involves several cell types, including $CD4^+$ Th2 cells, eosinophils, and mast cells (1). The immunopathogenic role of Th2 cells is suggested by the roles of their products, such as IL-4, IL-5, and IL-13 in the recruitment and activation of the primary effector cells of the allergic response, eosinophils and mast cells. Activation of these cells results in the release of many inflammatory mediators that seem to induce AHR individually or coordinately (2, 3), although the precise molecular mechanisms predisposing to the development of AHR in asthmatics are largely unknown. The hypothesis that airway inflammation is responsible for AHR is based on the finding of a significant relationship between the parameters of airway inflammation and AHR (4, 5) and on the observation that inhaled steroids reduce both airway inflammation and AHR (6, 7). However, a number of studies in asthmatic patients have cast doubt on the requirement of airway inflammation for AHR (see review in Ref. 8). In addition, dissociation of AHR from airway inflammation has also been reported in some mouse models of asthma, because IL-5-deficient BALB/c mice partially developed AHR by OVA sensitization/challenge in the absence of airway inflammation (9). Conversely, IL-10-deficient C57BL/6 mice failed to develop AHR even in the presence of robust airway inflammation (10).

Platelet-activating factor (PAF; 1-*O*-alkyl-2-acetyl-*sn*-glycero-3-phosphocholine) is a potent phospholipid mediator with various biological activities besides platelet activation (11). PAF acts by binding to a G protein-coupled seven-transmembrane receptor (12–16). PAF has long been implicated in the pathophysiological mechanisms of asthma (17), because exogenous PAF closely mimics many of the clinical features of asthma, including AHR (18, 19), bronchoconstriction (18), tracheal fluid secretion (20), and airway microvascular leakage (21) in animals and humans. PAF is detected in bronchoalveolar lavage (BAL) fluid from asthmatic patients but not from nonallergic subjects (22). Eosinophils and mast cells activated in asthmatic airways may be the cellular origins of PAF, because these cells are known to produce PAF in response to various stimuli in vitro (23, 24). Furthermore, PAF was reported to be a potent chemotactic factor for eosinophils (25) and to induce eosinophil degranulation in vitro (26). By using PAF receptor-deficient ($pafr^{-/-}$) and PAF receptor-overexpressing mice, we have previously demonstrated that PAF plays a critical role in anaphylaxis and acute injury in the lung (27, 28), suggesting that PAF mediates early-phase responses of allergy and inflammation in the tissue. However, the importance of PAF in the development of the allergen-induced AHR and chronic inflammation associated with asthma has not yet been investigated in $pafr^{-/-}$ mice. To define the role of PAF in the late-phase responses of allergy, we used an established murine asthma model, where mice were immunized with aluminum hydroxide adjuvant-adsorbed OVA and challenged with aerosolized OVA. In this study, we describe that $pafr^{-/-}$ mice, sensitized and challenged with OVA, displayed reduced AHR despite a significant eosinophilic airway inflammatory response. PAF may contribute to AHR in asthmatics independently of the eosinophilic airway inflammation.

Materials and Methods

Mice

$pafr^{-/-}$ mice were produced on a mixed C57BL/6 × 129/Ola genetic background as described previously (27). In the present study, $pafr^{-/-}$ mice and

Departments of *Biochemistry and Molecular Biology, †Respiratory Medicine, and ‡Geriatric Medicine, Faculty of Medicine, University of Tokyo, Tokyo, Japan; and §Core Research for Evolutional, Science and Technology, Japan Science and Technology Agency, Saitama, Japan

Received for publication August 26, 2003. Accepted for publication March 26, 2004.

The costs of publication of this article were defrayed in part by the payment of page charges. This article must therefore be hereby marked *advertisement* in accordance with 18 U.S.C. Section 1734 solely to indicate this fact.

[1] This work was supported in part by Grants-in-Aid from the Ministry of Education, Science, Culture, Sports and Technology of Japan (to T.S., T.N., and S.I.), Grants-in-Aid for Comprehensive Research on Aging and Health (to T.N. and S.I.) and for Research on Allergic Disease and Immunology (to S.I.) from the Ministry of Health, Labour and Welfare of Japan, and also grants from the Yamanouchi Foundation for Research on Metabolic Disorders (to T.N. and S.I.), the Kanae Foundation for Life and Socio-medical Science, and the Uehara Memorial Foundation (to S.I.).

[2] Address correspondence and reprint requests to Dr. Satoshi Ishii, Department of Biochemistry and Molecular Biology, Faculty of Medicine, University of Tokyo, 7-3-1 Hongo, Bunkyo, Tokyo 113-0033, Japan. E-mail address: mame@m.u-tokyo.ac.jp

[3] Abbreviations used in this paper: AHR, airway hyperresponsiveness; PAF, platelet-activating factor; BAL, bronchoalveolar lavage; LT, leukotriene; PAS, periodic acid-Schiff; R_L, total lung resistance; $EC_{200}R_L$, effective concentration of methacholine required to double the basal R_L.

0022-1767/04/$02.00

the corresponding wild-type ($pafr^{+/+}$) control mice have been backcrossed for 6–10 generations onto a BALB/c genetic background. The animals were maintained in a light-dark cycle with light from 7:00 a.m. to 8:00 p.m. at 22°C. Mice were fed with a standard laboratory diet and water ad libitum. All of the mice in this study were used under a protocol approved by the University of Tokyo Ethics Committee for Animal Experiments.

During the course of the backcrossing, we selected mice homozygous for the intact allele of the group IIA phospholipase A_2 gene that is linked to the PAF receptor gene on murine chromosome 4 (29, 30). The genetic distance between these genes is ~4.3 cM. Both C57BL/6 and 129/Ola inbred mice are deficient in group IIA phospholipase A_2 due to a congenital disruption of the gene, whereas BALB/c inbred mice have an intact gene for group IIA phospholipase A_2 (29, 31). Thus, our selection was able to exclude the possible effects of group IIA phospholipase A_2 deficiency, which may cause an abnormal metabolism of PAF, on the phenotypes of $pafr^{-/-}$ mice. For genotyping by PCR, genomic DNAs were isolated from tail biopsies. The PCR for PAF receptor alleles was performed with 10 pmol of each primer and 2.5 U of KOD Dash DNA polymerase (Toyobo, Osaka, Japan) in a 50-μl final volume. The PCR profile involved a 2-min denaturation step at 94°C, followed by 35 cycles of denaturation at 98°C for 10 s, annealing at 65°C for 2 s, and extension at 74°C for 30 s. The primers were as follows: forward, 5′-TATGGCTGACCTGCTCTTCCT GAT-3′, and reverse, 5′-TATTGGGCACTAGGTTGGTGGAGT-3′, for detecting the intact PAF receptor allele; and forward, 5′-GCCTGCTTGCCG AATATCATGGTGGAAAAT-3′, and reverse, 5′-AGGATGCAGTAGC CACAATGGATAC-3′, for detecting the disrupted PAF receptor allele. The former set of primers amplified a 287-bp DNA fragment, and the latter PCR product consisted of ~900 bp. The PCR for group IIA phospholipase A_2 alleles was performed with 10 pmol of each primer and 1.0 U of Ex *Taq*DNA polymerase (Takara, Kyoto, Japan) in a 40-μl final volume. The PCR profile involved a 2-min denaturation step at 94°C, followed by 35 cycles of denaturation at 95°C for 30 s, and annealing and extension at 65°C for 3 min. The primers were as follows: forward, 5′-TGTACCTGT CCTTCACAGAGCTGAC-3′, and reverse, 5′-TCCACTTTTCTCCAGG CGCTTGTAGC-3′, producing 673- and 674-bp DNA fragments from genomic DNA with the intact or mutant allele, respectively. *Hin*fI digestion of the PCR products produced polymorphic fragments of 291, 267, and 115 bp with the intact allele or 368, 191, and 115 bp with the mutant allele. The DNA fragments were detected by 2% agarose gel electrophoresis, and ethidium bromide staining.

Experimental design

Male and female mice at the age of 8–15 wk were used. Within each experimental group, the sex ratio and the backcross generation were equal, and the age did not differ significantly.

Sensitization and challenge protocol

Eosinophilic pulmonary inflammation was induced according to the method of Foster et al. (32) with slight modifications. Briefly, mice were sensitized on days 0 and 14 by i.p. injection of 50 μg of OVA (grade V; Sigma-Aldrich, St. Louis, MO)/1 mg of aluminum hydroxide (Imject Alum; Pierce, Rockland, IL) in 200 μl of 0.9% sterile saline (Otsuka, Tokyo, Japan). Nonsensitized mice received only 1 mg of aluminum hydroxide in 0.9% pyrogen-free saline. On day 23, the sensitized mice were exposed three times at 1-h intervals to an aerosol of OVA (10 mg/ml) in 0.9% saline for 30 min. The nonsensitized mice received saline only. The aerosol with a mass median diameter of 3.8 μm was generated at 20 l/min by a nebulizer (Pariboy; Pari, Starnberg, Germany) into a plastic desiccator of 19 liters, whose internal pressure was maintained at atmospheric pressure by an aspirator. The aerosol challenge protocol was then repeated every second day thereafter for 8 days. Mice were studied 16–22 h after the last aerosol challenge.

Serum and BAL fluid samples

For the collection of blood and BAL fluid, mice were anesthetized with 1.5 g of urethane per kilogram of body weight by an i.p. injection at a volume of 10 ml/kg, and placed in the supine position. The blood was taken by cutting the femoral vein and artery. The blood sample was collected in a serum separator tube coated with a coagulant (Seraquick Super; Azwell, Osaka, Japan), and then allowed to clot at room temperature for 1 h. The serum was recovered by centrifugation at 2,000 rpm for 10 min at room temperature. After a subsequent centrifugation at 12,000 rpm for 10 min at 4°C in a microcentrifuge, the supernatant was stored at −80°C until use.

Once bleeding had ceased, the trachea of a tracheostomized mouse was cannulated with an 18-gauge metal cannula with a beveled tip. After opening of the thorax by a wide incision of the diaphragm, the lung was lavaged twice with 1 ml of Ca^{2+}- and Mg^{2+}-free PBS containing a proteinase inhibitor mixture (Complete; Roche, Mannheim, Germany) at room temperature. The initial lavage was instilled and retrieved one time, whereas the second lavage was instilled twice. This procedure allowed for a greater number of lung washes with less diluent. In total, ~1.6 ml of BAL fluid was consistently recovered. The sample was centrifuged at 1000 rpm for 10 min at 4°C, and the supernatant was collected and stored at −80°C. The cell pellet was resuspended in 200–250 μl of cold saline containing 0.1% fatty acid-free BSA (Serologicals Proteins, Kankakee, IL). After an appropriate dilution (2- to 20-fold) of the cell suspension with Turk solution (Mutoh Chemical, Tokyo, Japan), the total cell number was counted with a hemocytometer. Slides of BAL fluid cells were prepared by placing 3×10^5 cells into a cytocentrifuge (Cytospin 3; Shandon, Pittsburgh, PA) at 350 rpm for 2 min, and staining with Diff-Quik (International Reagents, Kobe, Japan). The percentages of eosinophils, lymphocytes, macrophages/monocytes, and neutrophils were determined by counting their number in randomly selected areas, and dividing these numbers by the total cell count (at least 300 cells).

Determination of Ab levels in serum

The total IgE, and OVA-specific IgE and IgG1 levels in appropriately diluted sera were measured by ELISA as previously described (27). The lower limit of detection for total IgE was 50 ng/ml.

Determination of cytokine and cysteinyl leukotriene levels in BAL fluid

The concentrations of cytokines in the BAL fluid were determined using murine ELISA kits obtained from Endogen (Woburn, MA) for IL-4 and IL-5, and R&D Systems (Minneapolis, MN) for IL-13. Whole-lung samples were homogenized on ice using a rotor/stator type tissue homogenizer (Physcotron; Microtec, Chiba, Japan) for 40 s in 8 ml of PBS containing the proteinase inhibitor mixture per gram of lung tissue. After centrifugation at 18,000 × *g* for 10 min, the resulting supernatants were stored at −80°C until use. The lower limits of detection for IL-4, IL-5, and IL-13 were 5.0, 5.0, and 1.5 pg/ml, respectively. The total level of cysteinyl leukotrienes (LTC_4, LTD_4, and LTE_4) in the BAL fluid was evaluated by an enzyme immunoassay kit from Amersham (Piscataway, NJ). The lower limit of detection was 15 pg/ml.

Lung histology

After the blood collection, the lungs were removed and fixed in 10% phosphate-buffered formalin. From the paraffin-embedded right and left lobes of lung, three sections of 3-μm thickness were prepared at the upper, middle, and lower positions of each lobe, and stained with either H&E or periodic acid-Schiff (PAS). A semiquantitative scoring system was used to grade the size of lung infiltrates in the H&E-stained sections, where +5 signifies a widespread infiltrate around the majority of vessels and bronchioles, and +1 signifies a small number of inflammatory foci. The total lung score represents the sum of the scores of both lobes. The goblet cell hyperplasia in the PAS-stained sections was graded by a semiquantitative scoring system (0 = <5% goblet cells in airway epithelium; 1 = 5–25%; 2 = 25–50%; 3 = 50–75%; 4 = >75%) as performed by McMillan et al. (33). The sum of the airway scores from right lobe was divided by the number of airways examined (16–29 per mouse), and expressed as PAS score in arbitrary units. For both semiquantitative scoring, randomized and blinded slides were graded by S.I.

Measurement of airway responsiveness

A separate group of mice was anesthetized with a mixture of ketamine and pentobarbital (35 mg/kg each) by i.p. injection. A metal cannula was inserted into the trachea of a tracheostomized mouse. The total lung resistance (R_L) of a mechanically ventilated mouse was measured as previously described (34). Saline and methacholine (acetyl-β-methylcholine chloride; Wako, Osaka, Japan) were inhaled at a positive end-expiratory pressure of 3 cmH_2O. At the start of the protocol, two deep inhalations (3-fold the tidal volume) were delivered to standardize the volume history. All animals were then challenged with the saline aerosol for 2 min. The aerosol was generated with an ultrasonic nebulizer (Ultra-Neb100; DeVilbiss, Somerset, PA) and delivered through the inspiratory line into the trachea. Measurements of 10-s duration were made during the tidal ventilation beginning 1 min after the administration of the saline aerosol. This represented the baseline measurement. Subsequently, each dose of the methacholine aerosol was administered for 2 min in a dose-response manner (0.3125, 0.625, 1.25, 2.5, 5.0, 10, and 20 mg/ml saline). During the experiments, oxygen gas was continuously supplied to the ventilatory system. Airway responsiveness was assessed as the effective concentration of methacholine

Table I. *Total cell and differential counts obtained from BAL fluid*[a]

Treatment	n	Total Cell Counts ($\times 10^5$)	Differential Counts (% Total Cells)			
			Eosinophils	Lymphocytes	Macrophages	Neutrophils
pafr$^{+/+}$ SAL	4	1.6 ± 0.1	0.0 ± 0.0	2.7 ± 1.5	97.2 ± 1.5	0.1 ± 0.0
pafr$^{-/-}$ SAL	4	2.0 ± 0.1	0.0 ± 0.0	2.6 ± 1.2	97.0 ± 1.4	0.3 ± 0.2
pafr$^{+/+}$ OVA	7	40.9 ± 6.3	69.1 ± 3.0	17.7 ± 2.3	12.2 ± 1.9	1.0 ± 0.2
pafr$^{-/-}$ OVA	7	47.3 ± 4.1	63.5 ± 1.4	21.0 ± 2.0	13.7 ± 1.3	1.7 ± 0.5

[a] Data are the means ± SEM. SAL, Saline-immunized and saline-aerosolized treatment; OVA, OVA-immunized and OVA-aerosolized treatment. After BAL, the recovered cells were counted, and a portion of the cells were centrifuged onto microscope slides using a cytocentrifuge. The slides were stained with Diff-Quik, and differential cell counts were obtained. For the total cell counts and the percentages of the designated cell types, no significant differences were found between *pafr*$^{+/+}$ OVA and *pafr*$^{-/-}$ OVA mice (*t* test).

required to double the basal R_L ($EC_{200}R_L$), which was calculated by interpolation.

Binding assay for muscarinic receptors

Each membrane fraction was prepared from four lung tissues of two male and two female mice as previously described (35). The binding assays were performed in triplicate using 100 μg of membrane protein.

Statistical analysis

Mann-Whitney's *U* test (for nonparametric analysis) or unpaired *t* test (for parametric analysis) was used to determine the levels of difference between two groups. A value of $p < 0.05$ was considered to have statistical significance. For four groups, the difference was evaluated by ANOVA. When the ANOVA showed significant differences, pairwise comparisons were tested by Bonferroni-Dunn posthoc test, where $p < 0.0083$ was considered to be significant. All statistical calculations were performed with StatView-J, version 5.0 (Abacus Concepts, Berkeley, CA). The values for all measurements were expressed as the mean ± SEM.

Results

Serum Ig levels

In both *pafr*$^{+/+}$ and *pafr*$^{-/-}$ mice, aeroallergen challenge was associated with a significant increase in the serum levels of total and OVA-specific IgE, compared with their respective saline-treated controls (data not shown). However, there were no significant differences between *pafr*$^{+/+}$ and *pafr*$^{-/-}$ mice, when either the total or OVA-specific IgE level was compared. Similarly to the IgE levels, we found no difference in the OVA-specific IgG1 levels between *pafr*$^{+/+}$ and *pafr*$^{-/-}$ mice (data not shown).

Inflammatory cell recruitment in BAL fluid

The recovery of cells from the BAL fluid of saline-aerosolized *pafr*$^{+/+}$ and *pafr*$^{-/-}$ mice revealed a predominance of alveolar macrophages in both groups, without any significant difference between the numbers (Table I). Aerosol challenge of mice with OVA induced a drastic increase in the total cell number compared with mice given aerosolized saline (Table I). Differential cell counts revealed that the infiltrates in both genotypes were mainly composed of eosinophils. However, the total numbers of cells and the proportions of eosinophils, lymphocytes, macrophages/monocytes, and neutrophils did not differ between *pafr*$^{+/+}$ and *pafr*$^{-/-}$ mice given OVA (Table I). These data imply that *pafr*$^{-/-}$ mice were capable of recruiting significant numbers of inflammatory cells into the airway lumen after OVA challenge in a manner similar to *pafr*$^{+/+}$ mice.

Th2 cytokine and cysteinyl leukotriene levels in BAL fluid

We assessed the levels of the Th2 cytokines IL-4, IL-5, and IL-13 in the BAL fluid (Table II). In saline-treated mice of either genotype, the levels of the Th2 cytokines were near or below the limit of detection. Aeroallergen-challenged *pafr*$^{+/+}$ and *pafr*$^{-/-}$ mice showed elevated levels of the Th2 cytokines in the BAL fluid compared with their respective nonsensitized controls. Although there were trends toward higher levels of all three Th2 cytokines in *pafr*$^{+/+}$ mice compared with *pafr*$^{-/-}$ mice, these differences did not reach statistical significance ($p = 0.10$ for IL-4, $p = 0.20$ for IL-5, and $p = 0.12$ for IL-13; Mann-Whitney's *U* test). Whole-lung homogenates of the allergen-challenged mice also contained similar levels of IL-5 and IL-13 in both genotypes ($p = 0.87$ for IL-5, and $p = 0.07$ for IL-13; Mann-Whitney's *U* test). Next, the total level of cysteinyl leukotrienes (LTC_4, LTD_4, and LTE_4) in the BAL fluid was evaluated (Table II), because these lipid mediators are also involved in airway inflammation in mice as well as humans (36–38). In saline-treated mice of either genotype, the levels of cysteinyl leukotrienes were below the limit of detection. Aeroallergen challenge resulted in comparable elevation of the cysteinyl leukotriene levels in *pafr*$^{+/+}$ and *pafr*$^{-/-}$ mice ($p = 0.38$, *t* test).

Lung histology

The lung tissue fixed after OVA inhalation revealed dense peribronchial and perivascular accumulation of inflammatory cells as well as gross alterations in the structural integrity of the airway walls (Fig. 1, *B* and *D*). However, semiquantitative grading of the

Table II. *Th2 cytokine and cysteinyl leukotriene levels in lung*[a]

Treatment	BAL Fluid (pg/ml)					Lung Homogenate (pg/g lung)		
	IL-4	IL-5	IL-13	Cysteinyl leukotrienes	n	IL-5	IL-13	n
pafr$^{+/+}$ SAL	12.0 ± 3.8	5.0 ± 0.0	1.5 ± 0.0	15 ± 0	4	ND	ND	
pafr$^{-/-}$ SAL	9.1 ± 0.9	5.0 ± 0.0	2.2 ± 0.5	15 ± 0	4	ND	ND	
pafr$^{+/+}$ OVA	66.4 ± 15.4	53.8 ± 19.9	248.0 ± 45.2	239 ± 45	10	393 ± 32	2152 ± 203	13
pafr$^{-/-}$ OVA	32.7 ± 5.7	20.7 ± 6.0	156.4 ± 30.2	192 ± 26	10	388 ± 27	1747 ± 101	14

[a] Data are the means ± SEM. *pafr*$^{+/+}$, Wild-type mice; *pafr*$^{-/-}$, PAF receptor-deficient mice; SAL, saline-immunized and saline-aerosolized treatment; OVA, OVA-immunized OVA-aerosolized treatment. BAL fluid and whole-lung homogenate were centrifuged, and the resulting supernatant was subjected to ELISA. There was no significant difference between *pafr*$^{+/+}$ OVA and *pafr*$^{-/-}$ OVA mice (Mann-Whitney's *U* test) in any mediators. The lower limits of detection for IL-4, IL-5, IL-13, and cysteinyl leukotrienes were 5.0, 5.0, 1.5, and 15 pg/ml, respectively.

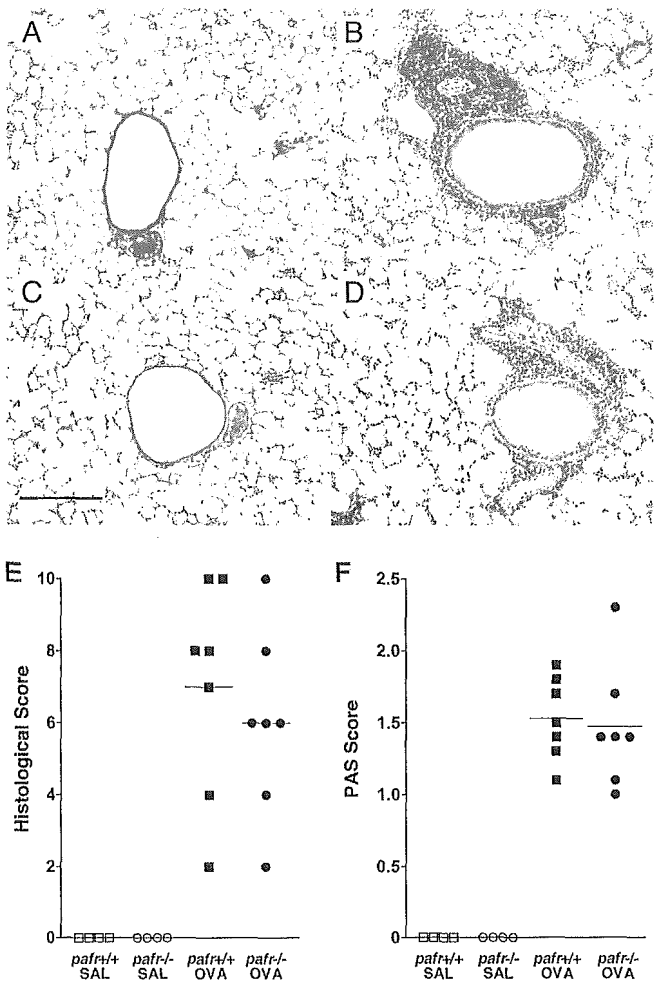

FIGURE 1. Histological analysis of lung sections. *A*, Nonsensitized $pafr^{+/+}$ mice exposed to an aerosol of saline. *B*, Sensitized $pafr^{+/+}$ mice exposed to OVA. *C*, Nonsensitized $pafr^{-/-}$ mice exposed to saline. *D*, Sensitized $pafr^{-/-}$ mice exposed to OVA. The H&E-stained sections shown are representative of six lung sections per mouse, from four or seven mice in each saline-treated or OVA-treated group, respectively. Scale bar, 200 μm. *E* and *F*, Assessments of lung inflammation. The stained sections were semiquantitatively scored as described in *Materials and Methods*, and scores for individual mice are presented. Bars depict means of groups. After aeroallergen challenge, $pafr^{-/-}$ mice develop lung inflammation at a comparable level to $pafr^{+/+}$ mice, as determined in sections stained with H&E (*E*). The levels of OVA-induced mucus production in $pafr^{+/+}$ and $pafr^{-/-}$ mice are identical, as determined in sections stained with PAS (*F*).

sections failed to elucidate a significant difference in the degree of airway inflammation between $pafr^{+/+}$ and $pafr^{-/-}$ mice (p = 0.34, Mann-Whitney's *U* test; Fig. 1*E*). Similarly, as shown in Fig. 1, *A* and *C*, the histological findings after saline treatment were unremarkable, with no observable differences between $pafr^{+/+}$ and $pafr^{-/-}$ mice (score: 0 in *E*). Excessive production of airway mucus glycoproteins by goblet cells in airway epithelium is a consistent finding in the lung of asthmatics. Semiquantification of goblet cells stained with PAS revealed similar mucus scores in $pafr^{-/-}$ mice compared with $pafr^{+/+}$ mice (Fig. 1*F*). Taken together, these results suggest that airway inflammation and goblet cell hyperplasia fully occurs in the absence of the PAF signaling.

Airway responsiveness

To assess aeroallergen-induced physiologic changes, both baseline R_L and airway responsiveness to an inhaled spasmogen, methacholine, were determined. Several aeroallergen-challenged mice had an increased baseline R_L compared with mice treated with saline. However, when analyzed as a group, aeroallergen-challenged mice exhibited no significant difference in the basal R_L in either saline-treated $pafr^{+/+}$ mice (0.55 ± 0.06 vs 0.39 ± 0.05 cmH_2O/ml/s; p = 0.09, ANOVA with Bonferroni-Dunn test) or saline-treated $pafr^{-/-}$ mice (0.50 ± 0.06 vs 0.40 ± 0.04 cmH_2O/ml/s; p = 0.30) (Fig. 2*A*). The inhalation of methacholine showed that $pafr^{+/+}$ mice aerosolized with OVA developed AHR compared with $pafr^{+/+}$ mice treated with aerosolized saline, because OVA-treated $pafr^{+/+}$ mice required a significantly lower dose of methacholine to achieve a 100% increase of the baseline R_L ($EC_{200}R_L$) than saline-treated $pafr^{+/+}$ mice ($\log EC_{200}R_L$ = −0.15 ± 0.09 vs 1.01 ± 0.12; $p < 0.0001$, ANOVA with Bonferroni-Dunn test) (Fig. 2*B*). Likewise, aerosol challenge of $pafr^{-/-}$ mice with OVA induced a significantly greater responsiveness to methacholine challenge compared with $pafr^{-/-}$ mice given saline ($\log EC_{200}R_L$ = 0.55 ± 0.16 vs 1.13 ± 0.08; p =

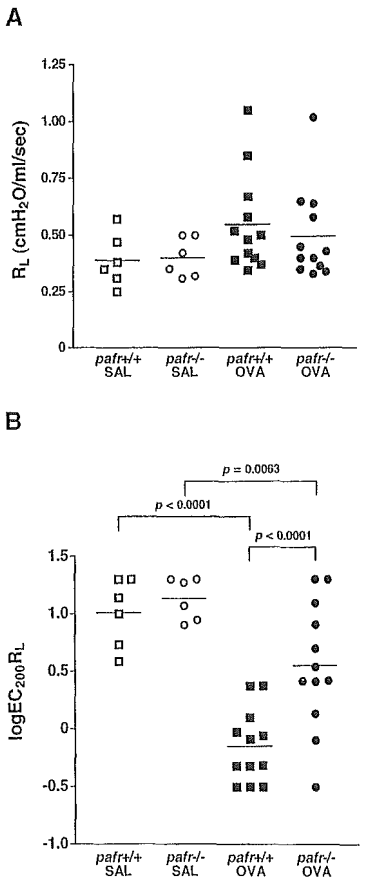

FIGURE 2. PAF receptor-regulated development of AHR in sensitized and aeroallergen-challenged mice. *A*, Baseline R_L. SAL, Saline-immunized and saline-aerosolized treatment; OVA, OVA-immunized and OVA-aerosolized treatment. Values for individual mice are presented. Bars depict means of groups. Before methacholine inhalation, no significant differences were observed among the four groups despite a nonsignificant trend toward an increased baseline R_L in the aeroallergen-challenged groups. *B*, Airway responsiveness to methacholine. Airway responsiveness was assessed by $EC_{200}R_L$. The logarithmic values of $EC_{200}R_L$ for individual mice are presented. Bars depict the means of the groups. $pafr^{-/-}$ OVA mice have significantly lower responsiveness to methacholine than $pafr^{+/+}$ OVA ($p < 0.0001$, ANOVA with Bonferroni-Dunn test). OVA-challenged $pafr^{+/+}$ and $pafr^{-/-}$ mice were significantly more responsive than their respective saline-treated controls ($p < 0.0001$ and p = 0.0063, respectively).

0.0063), but lower responsiveness than $pafr^{+/+}$ mice given OVA ($p < 0.0001$). These findings indicate that aeroallergen-induced AHR develops in $pafr^{-/-}$ mice to a significantly lower degree than $pafr^{+/+}$ mice.

Because methacholine is an agonist of muscarinic acetylcholine receptors, we examined the muscarinic receptor-binding activities of lung tissues from OVA-treated mice using a radiolabeled antagonist, [*N-methyl*-^{3}H]scopolamine. The lung membranes of $pafr^{+/+}$ and $pafr^{-/-}$ mice aerosolized with OVA bound similar amounts of this nonselective antagonist (Fig. 3), indicating comparable expression of muscarinic receptor-binding activity (B_{max} = 42.7 ± 2.7 and 44.8 ± 1.8 fmol/mg protein, respectively; $n = 3$; $p = 0.54$, t test). The binding was saturable with similar calculated K_d values of 237 ± 15 and 197 ± 19 pM ($n = 3$; $p = 0.16$, t test) in $pafr^{+/+}$ and $pafr^{-/-}$ mice, respectively.

Discussion

The murine asthma model recapitulates many of the features of human asthma, including the abundant eosinophilic and lymphocytic infiltration. PAF is chemotactic for eosinophils as well as macrophages/monocytes and neutrophils, all of which are also able to produce PAF (13, 14). Thus, it was reasonable to assume that PAF receptor may contribute to the induction of the airway inflammation associated with asthma. Unexpectedly, however, our studies indicate that the lack of PAF receptor did not alter the recruitment of inflammatory cells (i.e., total numbers of cells, or proportions of eosinophils, lymphocytes, macrophages/monocytes, and neutrophils) in the BAL fluid in this asthma model (Table I). Consistently, we found no significant histological differences in the degree of inflammation in the lung between $pafr^{+/+}$ and $pafr^{-/-}$ mice (Fig. 1). These data strongly suggest that PAF is dispensable for the airway inflammation, at least under our murine asthma model. Alternate chemoattractants, such as chemokines and leukotrienes (39–42), may recruit inflammatory cells to the airways. Indeed, BAL fluids from $pafr^{+/+}$ and $pafr^{-/-}$ mice contained comparable levels of cysteinyl leukotrienes, which are reported as important mediators for airway inflammation (36–38) (Table II). The present observations are consistent with our previous studies of thioglycolate-elicited peritoneal exudate macrophages (43), casein-elicited peritoneal exudate neutrophils (44), and acid-elicited neutrophils in the lung (28), where no differences were detected in cell numbers and differentials between $pafr^{+/+}$ and $pafr^{-/-}$ mice. However, another study of $pafr^{-/-}$ mice demonstrated diminished eosinophil recruitment in a murine model of allergic pleurisy where the s.c. sensitized mice were challenged once with OVA by intrapleural injection (45). The sensitization/challenge protocol of the pleurisy model is substantially different from that of the asthma model regarding route of Ag sensitization/challenge and frequency of Ag challenge; in this study, the i.p. sensitized mice were repeatedly challenged with OVA aerosols. Therefore, the lack of any differential recruitment of inflammatory cells in $pafr^{-/-}$ airways is likely due to the nature of the chronic inflammatory responses in the asthma model.

Elevated serum IgE levels have been reported to be important in the development of asthmatic responses (46, 47). Mice passively sensitized with IgG1 as well as IgE were reported to develop AHR and airway inflammation after allergen challenge (48). IL-4 and IL-5 are thought to be central to the development of asthmatic symptoms, because IL-5 regulates the differentiation, recruitment, and activation of eosinophils (49), and IL-4 drives IgE synthesis by B cells (50). Another Th2 cytokine, IL-13, is also hypothesized to play a pivotal role in the pathogenesis of asthma by activating B cells, eosinophils, and airway smooth muscle cells (51). OVA sensitization/challenge of $pafr^{-/-}$ mice resulted in serum Ab responses (data not shown) and airway Th2 responses (Table II). In all of these aspects, however, they were indistinguishable from $pafr^{+/+}$ controls. These findings suggest that a deficiency in PAF receptor did not affect the ability to induce humoral immune responses or Th2-directed cytokine responses to Ag.

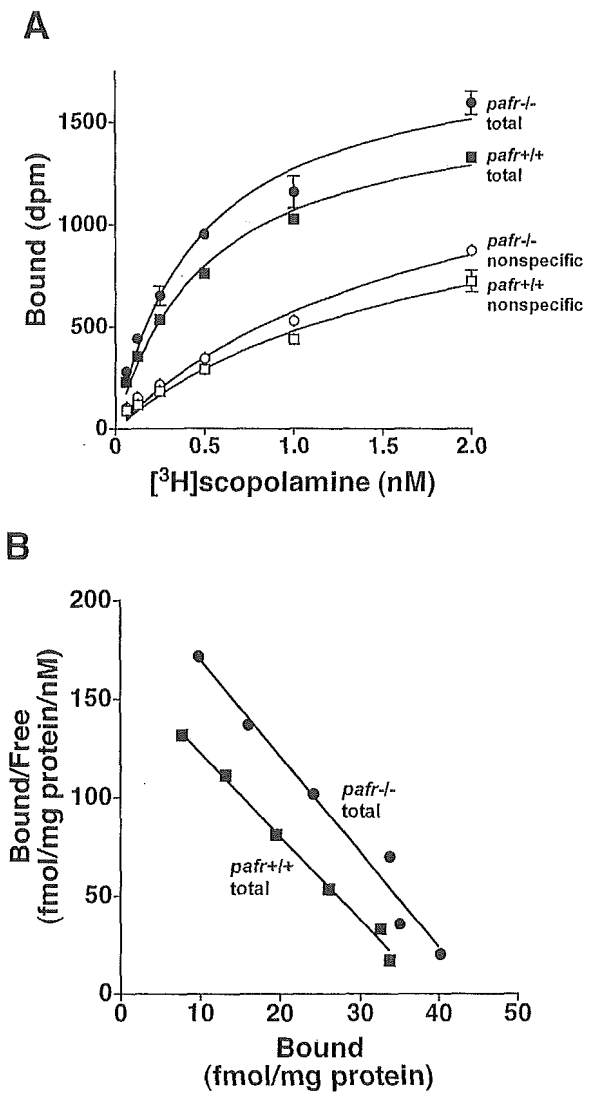

FIGURE 3. Muscarinic cholinergic receptor expression in lungs from sensitized and aeroallergen-challenged mice. *A*, [*N-methyl*-^{3}H]Scopolamine binding to lung membrane fractions. The lungs were excised and homogenized in a buffer, and the membrane fraction was prepared by ultracentrifugation. Aliquots of the resuspended membranes from $pafr^{+/+}$ and $pafr^{-/-}$ mice were incubated with increasing concentrations of [*N-methyl*-^{3}H]scopolamine for the detection of total binding. Nonspecific binding was determined by incubation in the presence of 20 μM methacholine. After incubation, free and bound antagonists were separated by rapid filtration on glass microfiber filters. Each point is the mean ± SEM of triplicate determinations, and the data are representative of three independent experiments. *B*, Scatchard analysis of the specific binding of [*N-methyl*-^{3}H]scopolamine to the lung membrane fractions shown in *A*. The specific binding was calculated as the difference between the total and nonspecific values. The data of $pafr^{+/+}$ and $pafr^{-/-}$ mice are shown. The mean values of K_d and B_{max} from the three independent experiments had no statistical significance between $pafr^{+/+}$ and $pafr^{-/-}$ mice given OVA (see *Results*).

AHR is a cardinal feature of asthma. PAF has been reported to induce AHR in animals and humans (18, 19), although the mechanisms are not fully understood. Moreover, we previously reported

that transgenic mice overexpressing PAF receptor showed AHR to inhaled methacholine under physiological conditions (52). To determine whether a lack of PAF receptor has an effect on the development of airway dysfunction, AHR was assessed in *pafr*$^{+/+}$ and *pafr*$^{-/-}$ mice. We found that *pafr*$^{-/-}$ mice had airway responsiveness similar to *pafr*$^{+/+}$ mice after saline-aerosolized treatment (Fig. 2*B*), indicating that the basal airway responsiveness is not different between *pafr*$^{+/+}$ and *pafr*$^{-/-}$ mice. Following Ag challenge, *pafr*$^{-/-}$ mice developed significantly increased airway responsiveness compared with their saline-treated controls. Furthermore, their responsiveness proved to be significantly lower than that of *pafr*$^{+/+}$ mice given OVA. Thus, PAF receptor is critical for the development of AHR following repeated aeroallergen challenge in sensitized mice, and AHR develops by PAF receptor-dependent and -independent pathways.

As reviewed by Drazen et al. (2) and Gali (3), two pathways involving mast cells and eosinophils have been elucidated to mediate aeroallergen-induced AHR. Recently, Hogan et al. (9) proposed a novel pathway to the development of AHR intimately mediated by CD4$^+$ T cells independently of IL-4 and IL-5, although the details of this pathway remain unknown. The relative contribution of these three cellular pathways to the induction of AHR is likely to be dependent on a number of factors including the strain of mouse, the choice of Ag, and the protocols for Ag sensitization and challenge, which may account for the apparent conflict observed among the mouse asthma models used by different investigators (9, 32, 39, 53–56). In the present study, we induced AHR in BALB/c mice with the procedure of Foster and coworkers (9, 32, 54, 57, 58) who have provided corroborative evidence of the important role of IgE, eosinophils, Th2 cytokines, and CD4$^+$ T cells. They immunized and boosted mice with OVA by i.p. injection of aluminum hydroxide-absorbed OVA, followed by repeated exposure to aerosolized OVA.

It is interesting that after such a strong sensitization/challenge procedure, little or no obligatory role of mast cells in AHR was observed in mast cell-deficient *W/W*^{v} mice (56, 59, 60). Consistently, AHR occurred normally with the sensitization/challenge procedure in IL-4-deficient BALB/c mice (9). Thus, in our study, the mast cell-dependent pathway could be excluded from the possible cellular mechanisms leading to the induction of AHR. Hence, it still remains unclear whether PAF is involved in the mast cell pathway. By using other procedures for sensitization/challenge to yield relatively attenuated airway responses, an even more pronounced contribution of PAF receptor to the mast cell pathway may be observed (56, 60).

pafr$^{-/-}$ mice, which have BALB/c genetic background, showed partially but significantly attenuated AHR despite a robust airway inflammation with infiltration of eosinophils and lymphocytes, indicating dissociation of AHR from airway inflammation in the mice. As described above, CD4$^+$ T cells regulate two distinct pathways that have been proposed to regulate aeroallergen-induced AHR; one is dependent on eosinophils, and another acts independently of IL-4 and IL-5. In BALB/c mice, the latter pathway is reported to play a major role in the development of AHR without eosinophilic inflammation and morphologic changes in the airways (9). Thus, it is possible that dissociation between AHR and airway inflammation observed in *pafr*$^{-/-}$ BALB/c mice is due to the involvement of PAF in the latter pathway. However, PAF also may be responsible for the development of AHR through the former (eosinophil) pathway. Although this lipid mediator was shown to be dispensable for eosinophil recruitment in this asthma model, it is possible that the infiltrated eosinophils in *pafr*$^{-/-}$ mice are not fully activated at the site of inflammation because of the lack of PAF stimulation. This is reminiscent of the results obtained in the murine acute lung injury model using *pafr*$^{-/-}$ mice in that PAF was essential for the activation of neutrophils but not for their recruitment (28).

The alternative possible target of PAF is smooth muscle. Our data demonstrate that the deficiency of PAF receptor is not associated with a detectable change in either the expression level (B_{max}) or ligand affinity (K_d) of muscarinic receptors in the lung, as measured by the nonspecific antagonist [*N-methyl*-^{3}H]scopolamine (Fig. 3). Although change of a minor pool of receptors cannot be ruled out, it is likely that the impaired muscarinic cholinergic response is due to a postreceptor event. PAF increases the susceptibility of smooth muscle to cholinergic stimulation, possibly by modulating the function of M_3 muscarinic receptor, a primary receptor for smooth muscle contraction (61). Indeed, we reported that the AHR to methacholine in transgenic mice overexpressing PAF receptor is mediated by a pathway sensitive to a PAF receptor antagonist (52). Similarly to the present data, the muscarinic receptor-binding activities (B_{max} and K_d) of the PAF receptor transgenic mice were indistinguishable from those of wild-type control mice (35). Because PAF receptor mRNA was detected in airway smooth muscle in human peripheral lung (62), it is possible for PAF to modulate the M_3 receptor-evoked smooth muscle contraction at the level of intracellular signal transduction. Whereas M_3 receptor on smooth muscle cells couples to phosphoinositol turnover through $G_{q/11}$ (61), PAF receptor is capable of coupling to $G_{i/o}$ and $G_{q/11}$ (14), suggesting a stimulatory cross talk between the intracellular signals from the two distinct receptors (63).

In most cases, AHR is strongly associated with airway inflammation (64–67), and anti-inflammatory drugs are currently used for bronchial asthma (6, 7). However, the PAF-mediated AHR appears to be independent of inflammation, because *pafr*$^{-/-}$ mice showed a reduction of AHR without diminishment of airway inflammation as shown in this study. This notion is further supported by our previous findings that the PAF receptor-overexpressing mice had AHR without obvious inflammatory responses (52). Recombinant plasma-type PAF acetylhydrolase abrogated airway responsiveness and inflammation concomitantly in a mouse asthma model (65). The apparent discrepancy between our data and those of the report may be attributed to the difference of sensitization procedure. In addition, it is notable that substrates for PAF acetylhydrolase and agonists for PAF receptor do not overlap completely (14, 68).

In summary, the present study demonstrates an important role for PAF receptor in the development of AHR after allergic sensitization/challenge in mice despite the normal expression density and ligand affinity of muscarinic cholinergic receptor. Furthermore, the airway inflammation was not affected by the absence of PAF receptor, suggesting that, as a complement anaphylatoxin C3a (69), PAF only acts downstream of the airway inflammation in bronchial asthma.

Acknowledgments

We thank Dr. N. Uozumi for the group IIA phospholipase A_2 genotyping. We are also grateful to R. Mitsuzono, M. Yoshino, C. Ohkawara, T. Sato, H. Shiozawa, Y. Tomizawa, and Y. Matsumoto for technical assistance.

References

1. Wills-Karp, M. 1999. Immunologic basis of antigen-induced airway hyperresponsiveness. *Annu. Rev. Immunol. 17:255.*
2. Drazen, J. M., J. P. Arm, and K. F. Austen. 1996. Sorting out the cytokines of asthma. *J. Exp. Med. 183:1.*
3. Galli, S. J. 1997. Complexity and redundancy in the pathogenesis of asthma: reassessing the roles of mast cells and T cells. *J. Exp. Med. 186:343.*
4. Bousquet, J., P. Chanez, J. Y. Lacoste, G. Barneon, N. Ghavanian, I. Enander, P. Venge, S. Ahlstedt, J. Simony-Lafontaine, P. Godard, and F. B. Michel. 1990. Eosinophilic inflammation in asthma. *N. Engl. J. Med. 323:1033.*
5. Robinson, D. S., A. M. Bentley, A. Hartnell, A. B. Kay, and S. R. Durham. 1993. Activated memory T helper cells in bronchoalveolar lavage fluid from patients

with atopic asthma: relation to asthma symptoms, lung function, and bronchial responsiveness. *Thorax 48:26.*
6. Barnes, P. J. 1989. A new approach to the treatment of asthma. *N. Engl. J. Med. 321:1517.*
7. Djukanovic, R., J. W. Wilson, K. M. Britten, S. J. Wilson, A. F. Walls, W. R. Roche, P. H. Howarth, and S. T. Holgate. 1992. Effect of an inhaled corticosteroid on airway inflammation and symptoms in asthma. *Am. Rev. Respir. Dis. 145:669.*
8. Brusasco, V., E. Crimi, and R. Pellegrino. 1998. Airway hyperresponsiveness in asthma: not just a matter of airway inflammation. *Thorax 53:992.*
9. Hogan, S. P., K. I. Matthaei, J. M. Young, A. Koskinen, I. G. Young, and P. S. Foster. 1998. A novel T cell-regulated mechanism modulating allergen-induced airways hyperreactivity in BALB/c mice independently of IL-4 and IL-5. *J. Immunol. 161:1501.*
10. Makela, M. J., A. Kanehiro, L. Borish, A. Dakhama, J. Loader, A. Joetham, Z. Xing, M. Jordana, G. L. Larsen, and E. W. Gelfand. 2000. IL-10 is necessary for the expression of airway hyperresponsiveness but not pulmonary inflammation after allergic sensitization. *Proc. Natl. Acad. Sci. USA 97:6007.*
11. Prescott, S. M., G. A. Zimmerman, D. M. Stafforini, and T. M. McIntyre. 2000. Platelet-activating factor and related lipid mediators. *Annu. Rev. Biochem. 69:419.*
12. Honda, Z., M. Nakamura, I. Miki, M. Minami, T. Watanabe, Y. Seyama, H. Okado, H. Toh, K. Ito, T. Miyamoto, and T. Shimizu. 1991. Cloning by functional expression of platelet-activating factor receptor from guinea-pig lung. *Nature 349:342.*
13. Izumi, T., and T. Shimizu. 1995. Platelet-activating factor receptor: gene expression and signal transduction. *Biochim. Biophys. Acta 1259:317.*
14. Ishii, S., and T. Shimizu. 2000. Platelet-activating factor (PAF) receptor and genetically engineered PAF receptor mutant mice. *Prog. Lipid Res. 39:41.*
15. Ishii, S., T. Nagase, and T. Shimizu. 2002. Platelet-activating factor receptor. *Prostaglandins Other Lipid Mediat. 68–69:599.*
16. Honda, Z., S. Ishii, and T. Shimizu. 2002. Platelet-activating factor receptor. *J. Biochem. 131:773.*
17. Barnes, P. J., K. F. Chung, and C. P. Page. 1998. Inflammatory mediators of asthma: an update. *Pharmacol. Rev. 50:515.*
18. Cuss, F. M., C. M. Dixon, and P. J. Barnes. 1986. Effects of inhaled platelet activating factor on pulmonary function and bronchial responsiveness in man. *Lancet 2:189.*
19. Kaye, M. G., and L. J. Smith. 1990. Effects of inhaled leukotriene D_4 and platelet-activating factor on airway reactivity in normal subjects. *Am. Rev. Resp. Dis. 141:993.*
20. Steiger, J., M. A. Bray, and N. Subramanian. 1987. Platelet activating factor (PAF) is a potent stimulator of porcine tracheal fluid secretion in vitro. *Eur. J. Pharmacol. 142:367.*
21. Evans, T. W., K. F. Chung, D. F. Rogers, and P. J. Barnes. 1987. Effect of platelet-activating factor on airway vascular permeability: possible mechanisms. *J. Appl. Physiol. 63:479.*
22. Stenton, S. C., E. N. Court, W. P. Kingston, P. Goadby, C. A. Kelly, M. Duddridge, C. Ward, D. J. Hendrick, and E. H. Walters. 1990. Platelet-activating factor in bronchoalveolar lavage fluid from asthmatic subjects. *Eur. Respir. J. 3:408.*
23. Schleimer, R. P., D. W. MacGlashan, Jr., S. P. Peters, R. N. Pinckard, N. F. Adkinson, Jr., and L. M. Lichtenstein. 1986. Characterization of inflammatory mediator release from purified human lung mast cells. *Am. Rev. Respir. Dis. 133:614.*
24. Cromwell, O., A. J. Wardlaw, A. Champion, R. Moqbel, D. Osei, and A. B. Kay. 1990. IgG-dependent generation of platelet-activating factor by normal and low density human eosinophils. *J. Immunol. 145:3862.*
25. Wardlaw, A. J., R. Moqbel, O. Cromwell, and A. B. Kay. 1986. Platelet-activating factor: a potent chemotactic and chemokinetic factor for human eosinophils. *J. Clin. Invest. 78:1701.*
26. Kroegel, C., T. Yukawa, J. Westwick, and P. J. Barnes. 1989. Evidence for two platelet activating factor receptors on eosinophils: dissociation between PAF-induced intracellular calcium mobilization degranulation and superoxides anion generation in eosinophils. *Biochem. Biophys. Res. Commun. 162:511.*
27. Ishii, S., T. Kuwaki, T. Nagase, K. Maki, F. Tashiro, S. Sunaga, W. H. Cao, K. Kume, Y. Fukuchi, K. Ikuta, et al. 1998. Impaired anaphylactic responses with intact sensitivity to endotoxin in mice lacking a platelet-activating factor receptor. *J. Exp. Med. 187:1779.*
28. Nagase, T., S. Ishii, K. Kume, N. Uozumi, T. Izumi, Y. Ouchi, and T. Shimizu. 1999. Platelet-activating factor mediates acid-induced lung injury in genetically engineered mice. *J. Clin. Invest. 104:1071.*
29. MacPhee, M., K. P. Chepenik, R. A. Liddell, K. K. Nelson, L. D. Siracusa, and A. M. Buchberg. 1995. The secretory phospholipase A_2 gene is a candidate for the *Mom1* locus, a major modifier of ApcMin-induced intestinal neoplasia. *Cell 81:957.*
30. Ishii, S., Y. Matsuda, M. Nakamura, I. Waga, K. Kume, T. Izumi, and T. Shimizu. 1996. A murine platelet-activating factor receptor gene: cloning, chromosomal localization and up-regulation of expression by lipopolysaccharide in peritoneal resident macrophages. *Biochem. J. 314:671.*
31. Kennedy, B. P., P. Payette, J. Mudgett, P. Vadas, W. Pruzanski, M. Kwan, C. Tang, D. E. Rancourt, and W. A. Cromlish. 1995. A natural disruption of the secretory group II phospholipase A_2 gene in inbred mouse strains. *J. Biol. Chem. 270:22378.*
32. Foster, P. S., S. P. Hogan, A. J. Ramsay, K. I. Matthaei, and I. G. Young. 1996. Interleukin 5 deficiency abolishes eosinophilia, airways hyperreactivity, and lung damage in a mouse asthma model. *J. Exp. Med. 183:195.*
33. McMillan, S. J., B. Bishop, M. J. Townsend, A. N. McKenzie, and C. M. Lloyd. 2002. The absence of interleukin 9 does not affect the development of allergen-induced pulmonary inflammation nor airway hyperreactivity. *J. Exp. Med. 195:51.*
34. Nagase, T., H. Kurihara, Y. Kurihara, T. Aoki, Y. Fukuchi, Y. Yazaki, and Y. Ouchi. 1998. Airway hyperresponsiveness to methacholine in mutant mice deficient in endothelin-1. *Am. J. Respir. Crit. Care Med. 157:560.*
35. Nagase, T., S. Ishii, H. Shindou, Y. Ouchi, and T. Shimizu. 2002. Airway hyperresponsiveness in transgenic mice overexpressing platelet activating factor receptor is mediated by an atropine-sensitive pathway. *Am. J. Respir. Crit. Care Med. 165:200.*
36. Eum, S. Y., K. Maghni, Q. Hamid, H. Campbell, D. H. Eidelman, and J. G. Martin. 2003. Involvement of the cysteinyl-leukotrienes in allergen-induced airway eosinophilia and hyperresponsiveness in the mouse. *Am. J. Respir. Cell Mol. Biol. 28:25.*
37. Nakamura, Y., M. Hoshino, J. J. Sim, K. Ishii, K. Hosaka, and T. Sakamoto. 1998. Effect of the leukotriene receptor antagonist pranlukast on cellular infiltration in the bronchial mucosa of patients with asthma. *Thorax 53:835.*
38. Coffey, M., and M. Peters-Golden. 2003. Extending the understanding of leukotrienes in asthma. *Curr. Opin. Allergy Clin. Immunol. 3:57.*
39. Humbles, A. A., B. Lu, D. S. Friend, S. Okinaga, J. Lora, A. Al-Garawi, T. R. Martin, N. P. Gerard, and C. Gerard. 2002. The murine CCR3 receptor regulates both the role of eosinophils and mast cells in allergen-induced airway inflammation and hyperresponsiveness. *Proc. Natl. Acad. Sci. USA 99:1479.*
40. Medoff, B. D., A. Sauty, A. M. Tager, J. A. Maclean, R. N. Smith, A. Mathew, J. H. Dufour, and A. D. Luster. 2002. IFN-γ-inducible protein 10 (CXCL10) contributes to airway hyperreactivity and airway inflammation in a mouse model of asthma. *J. Immunol. 168:5278.*
41. Henderson, W. R., Jr., D. B. Lewis, R. K. Albert, Y. Zhang, W. J. Lamm, G. K. Chiang, F. Jones, P. Eriksen, Y. T. Tien, M. Jonas, and E. Y. Chi. 1996. The importance of leukotrienes in airway inflammation in a mouse model of asthma. *J. Exp. Med. 184:1483.*
42. Irvin, C. G., Y. P. Tu, J. R. Sheller, and C. D. Funk. 1997. 5-Lipoxygenase products are necessary for ovalbumin-induced airway responsiveness in mice. *Am. J. Physiol. 272:L105.*
43. Ohshima, N., S. Ishii, T. Izumi, and T. Shimizu. 2002. Receptor-dependent metabolism of platelet-activating factor in murine macrophages. *J. Biol. Chem. 277:9722.*
44. Shindou, H., S. Ishii, N. Uozumi, and T. Shimizu. 2000. Roles of cytosolic phospholipase A_2 and platelet-activating factor receptor in the Ca-induced biosynthesis of PAF. *Biochem. Biophys. Res. Commun. 271:812.*
45. Klein, A., V. Pinho, A. L. Alessandrini, T. Shimizu, S. Ishii, and M. M. Teixeira. 2002. Platelet-activating factor drives eotaxin production in an allergic pleurisy in mice. *Br. J. Pharmacol. 135:1213.*
46. Burrows, B., F. D. Martinez, M. Halonen, R. A. Barbee, and M. G. Cline. 1989. Association of asthma with serum IgE levels and skin-test reactivity to allergens. *N. Engl. J. Med. 320:271.*
47. Sears, M. R., B. Burrows, E. M. Flannery, G. P. Herbison, C. J. Hewitt, and M. D. Holdaway. 1991. Relation between airway responsiveness and serum IgE in children with asthma and in apparently normal children. *N. Engl. J. Med. 325:1067.*
48. Oshiba, A., E. Hamelmann, K. Takeda, K. L. Bradley, J. E. Loader, G. L. Larsen, and E. W. Gelfand. 1996. Passive transfer of immediate hypersensitivity and airway hyperresponsiveness by allergen-specific immunoglobulin (Ig) E and IgG1 in mice. *J. Clin. Invest. 97:1398.*
49. Sanderson, C. J. 1992. Interleukin-5, eosinophils, and disease. *Blood 79:3101.*
50. Paul, W. E. 1991. Interleukin-4: a prototypic immunoregulatory lymphokine. *Blood 77:1859.*
51. Wills-Karp, M. 2000. Murine models of asthma in understanding immune dysregulation in human asthma. *Immunopharmacology 48:263.*
52. Ishii, S., T. Nagase, F. Tashiro, K. Ikuta, S. Sato, I. Waga, K. Kume, J. Miyazaki, and T. Shimizu. 1997. Bronchial hyperreactivity, increased endotoxin lethality and melanocytic tumorigenesis in transgenic mice overexpressing platelet-activating factor receptor. *EMBO J. 16:133.*
53. Corry, D. B., H. G. Folkesson, M. L. Warnock, D. J. Erle, M. A. Matthay, J. P. Wiener-Kronish, and R. M. Locksley. 1996. Interleukin 4, but not interleukin 5 or eosinophils, is required in a murine model of acute airway hyperreactivity. *J. Exp. Med. 183:109.*
54. Hogan, S. P., A. Mould, H. Kikutani, A. J. Ramsay, and P. S. Foster. 1997. Aeroallergen-induced eosinophilic inflammation, lung damage, and airways hyperreactivity in mice can occur independently of IL-4 and allergen-specific immunoglobulins. *J. Clin. Invest. 99:1329.*
55. MacLean, J. A., G. T. De Sanctis, K. G. Ackerman, J. M. Drazen, A. Sauty, E. DeHaan, F. H. Green, I. F. Charo, and A. D. Luster. 2000. CC chemokine receptor-2 is not essential for the development of antigen-induced pulmonary eosinophilia and airway hyperresponsiveness. *J. Immunol. 165:6568.*
56. Kobayashi, T., T. Miura, T. Haba, M. Sato, I. Serizawa, H. Nagai, and K. Ishizaka. 2000. An essential role of mast cells in the development of airway hyperresponsiveness in a murine asthma model. *J. Immunol. 164:3855.*
57. Webb, D. C., A. N. McKenzie, A. M. Koskinen, M. Yang, J. Mattes, and P. S. Foster. 2000. Integrated signals between IL-13, IL-4, and IL-5 regulate airways hyperreactivity. *J. Immunol. 165:108.*
58. Mattes, J., M. Yang, S. Mahalingam, J. Kuehr, D. C. Webb, L. Simson, S. P. Hogan, A. Koskinen, A. N. McKenzie, L. A. Dent, et al. 2002. Intrinsic defect in T cell production of interleukin (IL)-13 in the absence of both IL-5 and eotaxin precludes the development of eosinophilia and airways hyperreactivity in experimental asthma. *J. Exp. Med. 195:1433.*